Master Thesis

Towards New Molecular Glues for E3 Ligase DCAF16

by
Mira **Mayerl**

under the supervision of
Prof. Dr. Dennis **Gillingham**
Prof. Dr. Hannes **Mikula**
Dr. Giulia **Mancini**

conducted at
Department of Chemistry, University of Basel
Institute of Applied Synthetic Chemistry, Vienna University of Technology

Vienna, 01/08/2024

Abstract

In the last two decades, targeted protein degradation has emerged as a new therapeutic strategy whose success is attested by the large number of degraders that are currently in clinical studies. However, the successful degraders described so far, are almost exclusively based on E3 ligase Cereblon, while all of the other 600+ human E3 ligases are neglected. In general, E3 ligases exhibit a defined substrate specificity, thus, using new E3 ligases would enable to extend the scope of possible targets tremendously. Not only expanding the TPD toolbox, exploiting new E3 ligases will open the door for tissue or cell specific degradation too. DCAF16 is an E3 ligase that still remains insufficiently characterized, even though some degraders targeting DCAF16 are already described in the literature. One of those degraders is MMH1 from Li *et al.* that degrades the protein BRD4 by covalently binding DCAF16. Based on MMH1, the aim of this work was to develop a competition assay to find new covalent binders for DCAF16. First, probes were synthesized, which are meant to compete later on with potential new binders in the envisioned assay. The first probe B1, a derivative of MMH1 with an additional biotin moiety, was synthesized successfully. However, in cell studies it was not possible to confirm its interaction with DCAF16. Thus, a new probe, termed A1, was synthesized. Instead of the larger biotin moiety, A1 features an alkyne that allows copper-catalyzed azide–alkyne cycloadditions to install biotin or fluorophores later on for visualization of the binding event. Subsequently, A1 was confirmed to interact with DCAF16. After optimization of the click conditions, fluorescent labeling of DCAF16 with cyanine5.5-azide was achieved. The labeling was succeeded in both cases, in case of A1 treatment of cell lysates as well as A1 treatment of living HeLa cells. Especially as additional unspecific binding was observed, an important next step would be the validation of DCAF16 as target of A1. Although some fine-tuning remains to be done, this work lays the foundation for a new competition assay to find novel binders for the E3 ligase DCAF16.

Kurzfassung

Der gezielte Abbau von Proteinen unter Verwendung zelleigener Abbaumechanismen hat sich in den letzten zwei Jahrzehnten als neue therapeutische Strategie etabliert. Dass diese Strategie erfolgreich ist, kann an den vielen entsprechenden Medikamenten abgelesen werden, die sich derzeit in klinischen Studien befinden. Bislang nutzen diese Wirstoffmoleküle fast ausschließlich die E3 Ligase Cereblon um den Proteinabbau zu initiieren. Das menschliche Genom beinhaltet jedoch mehr als 600 E3 Ligasen, welche für den gezielten Abbau potentiell verwendet werden könnten. Da jede E3 Ligase höchst spezifisch in Bezug auf ihre Substrate ist, könnte durch die Verwendung neuer E3 Ligasen die Bandbreite möglicher Targets enorm erweitert werden. Weiters könnte die Spezifität von zukünftigen Medikamenten drastisch erhöht werden, da viele E3 Ligasen zell-, gewebe- und tumorspezifisch gehäuft auftreten. DCAF16 ist eine E3 Ligase, welche derzeit noch unzureichend charakterisiert ist. Einige abbauinitiierenden Moleküle die auf DCAF16 basieren, wurden in den letzten Jahren bereits erforscht, unter ihnen beispielsweise das kovalent bindende Molekül MMH1 von Li *et al.* Das Ziel der vorliegenden Arbeit war, einen Assay basierend auf MMH1 zu entwickeln, um neue Moleküle zu finden, die kovalent an DCAF16 binden. Dafür wurden zunächst Sondenmoleküle synthetisiert, die im Assay später mit neuen, potentiell an DCAF16 binden-den, Molekülen konkurrieren sollten. B1 war das erste erfolgreich hergestellte Sondenmolekül, es ist ein Derivat von MMH1, jedoch mit zusätzlicher Biotin-Funktionalität. Diese Funktionalität kann beispielsweise zur Visualisierung verwendet werden, um zu sehen ob das Molekül an DCAF16 bindet. Da in einem anschließenden Zellexperiment jedoch nicht validiert werden konnte, dass B1 mit DCAF16 interagiert, wurde ein neues Sondenmolekül, genannt A1, synthetisiert. Anstelle der raumeinnehmenden Biotin-Funktionalität besitzt A1 ein Alkin. Diese Gruppe ist nicht nur kleiner, sondern ermöglicht mithilfe einer kupferkatalysierte Azid-Alkin-Cycloaddition das spätere Hinzufügen von Biotin oder einem Fluorophor. Im Anschluss an die erfolgreiche Synthese konnte bestätigt werden, dass A1 mit DCAF16 interagiert. Nach der Optimierung der Bedingungen für die Click-Reaktion gelang es, DCAF16 mit Cyanin5.5-Azid zu markieren. Dies gelang sowohl nach der Inkubation von Zelllysat mit A1 als auch nach der Inkubation von lebenden HeLa-Zellen mit A1. Da in den entsprechenden Western Blots auch unspezifisches Binden von A1 beobachtet wurde, wird ein wichtiger nächster Schritt die Validierung von DCAF16 als Target von A1 sein. Obwohl noch einige Feinheiten untersucht werden müssen, legt diese Arbeit den Grundstein für einen neuen kompetitiven Assay, um neue Wirkstoffmoleküle zu finden, die an DCAF16 binden.

Acknowledgments

First of all, I would like to thank Dennis Gillingham and Hannes Mikula for giving me the opportunity to conduct my master thesis in this fascinating topic. Thank you Dennis for hosting me in your lab in Basel and thank you Hannes for supervising me from Vienna, I really appreciate the time you took throughout the process!

Special thanks to Giulia, who was there for me and all of my questions at any time. Thank you for your guidance and patience, I could really learn a lot from you during this time! I would also like to thank Pedro for sharing his lab and knowledge with me - I learned how to do western blots from the best teacher possible! Furthermore, I would like to thank the whole Gillingham group for welcoming me so warmly and for all the fun activities and the bouldering we did together. I really enjoyed the time with you!

Last but not least, I want to say thank you to my family and friends. Thank you all for your constant support - I am so happy to have you by my side!

Abbreviations

AcOH	acetic acid
ALS	autophagy-lysosome system
AUTAC	autophagy-targeting chimeras
Boc	*tert*-butyloxycarbonyl
BRD4	bromodomain-containing protein 4
CRBN	cereblon
CRL4	cullin-RING ubiquitin ligase 4
CuAAC	copper-catalyzed azide–alkyne cycloaddition
CUL4	cullin 4
CY5	cyanine5.5 dye
DCAF16	DDB1 and CUL4 associated factor 16
DCM	dichloromethane
DDB1	DNA damage-binding protein 1
DIPEA	*N,N*-diisopropylethylamine
DMEM	dulbecco's modified eagle's medium
DMF	dimethylformamid
DMSO	dimethyl sulfoxide
EDC	1-ethyl-3-carbodiimide
ESI-HRMS	electrospray ionization high resolution mass spectrometry
HATU	hexafluorophosphate azabenzotriazole tetramethyl uronium
HOBt	hydroxybenzotriazole
HPLC	high-performance liquid chromatography
LC-MS	liquid chromatography mass spectrometry
LYTAC	lysosome-targeting chimeras
MeOH	methanol
NMR	nuclear magnetic resonance
PBS	phosphate-buffered saline

PDB	protein data bank
PROTAC	proteolysis targeting chimera
RIPA buffer	radioimmunoprecipitation assay buffer
r.t.	room temperature
SAR	structure-activity relationship
SDS-PAGE	sodium dodecyl sulfate polyacrylamide gel electrophoresis
S-Phos	dicyclohexyl(2′,6′-dimethoxy[1,1′-biphenyl]-2-yl)phosphane
TBST	tris-buffered saline with tween
TFA	trifluoroacetic acid
THF	tetrahydrofurane
THPTA	tris(3-hydroxypropyltriazolylmethyl)amine
TLC	thin layer chromatography
TMSCl	trimethylsilyl chloride
TPD	targeted protein degradation
UHPLC-MS	ultra high-performance liquid chromatography mass spectrometry
UPS	ubiquitin-proteasome system
VHL	von Hippel-Lindau

General explanatory notes

Literature References

References to literature are distinguished as Arabic numerals in square brackets.

Substance Labeling

Compounds already described in literature are sequentially numbered in bold Arabic numerals. Commercially available reagents used “as bought” were not numbered. Compounds unknown to literature that were prepared in the course of this thesis are numbered in bold roman numerals.

Nomenclature

The nomenclature of chemical compounds which are not described in the literature is based on the rules of *Chemical Abstracts*. Compounds known to literature, reagents or solvents might be described by simplified terms, common or trade names.

Illustrations

Illustrations were created with BioRender.com.

Table of Contents

Chapter 1

Schemes

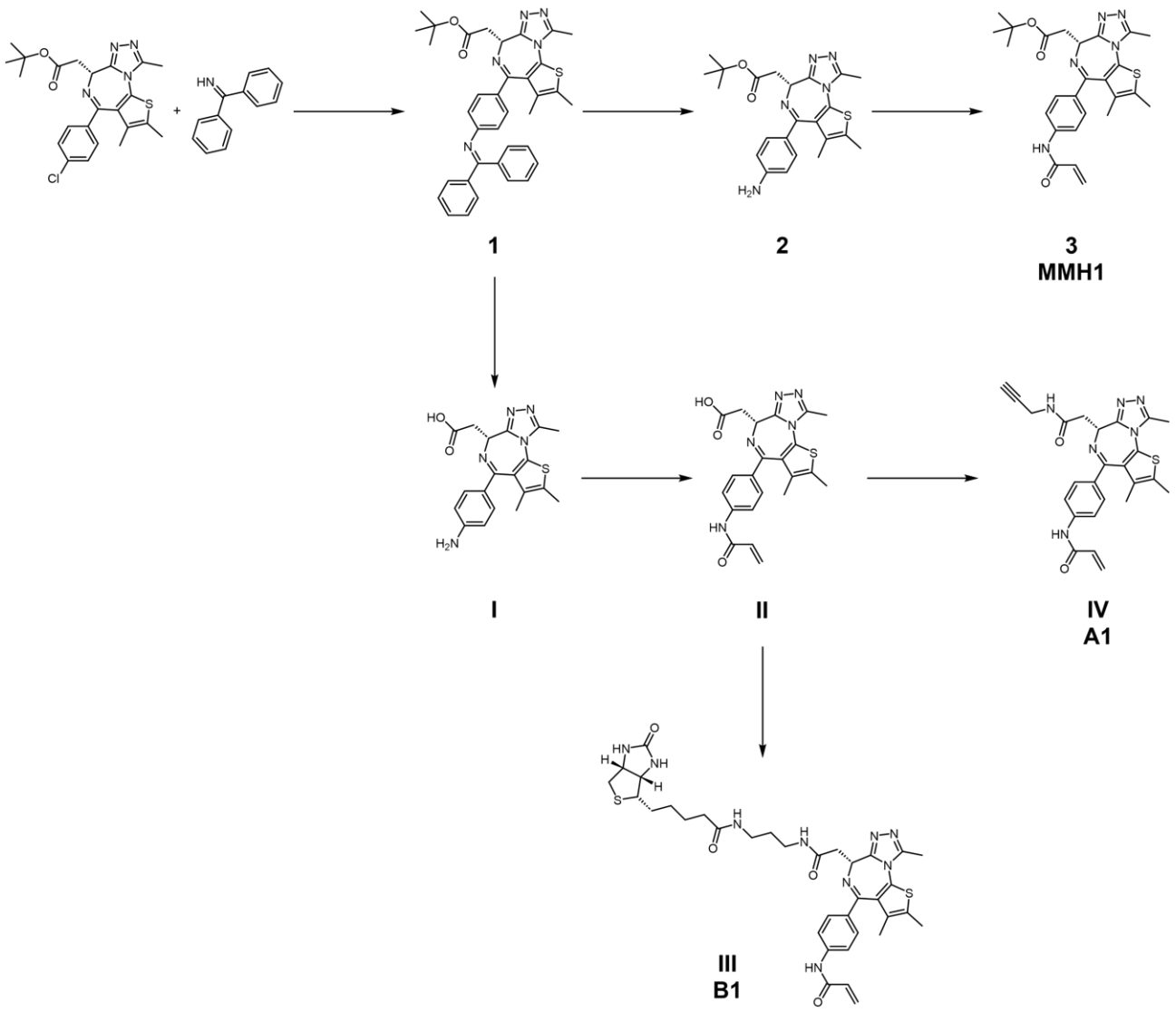

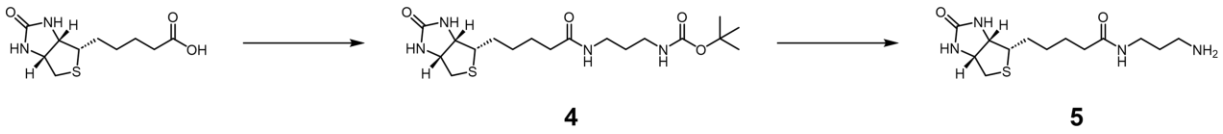

4 **5**

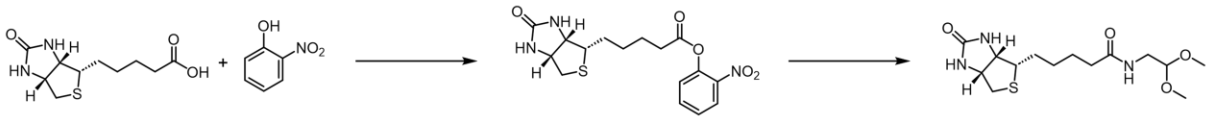

6 **7**

Chapter 2

Introduction

2.1 Targeted Protein Degradation

Over the last 20 years, targeted protein degradation (TPD) has become a promising therapeutic approach. In TPD, small molecules are used to reprogram the cells own protein disposal system to induce the degradation of therapeutic relevant proteins. The small molecule degraders act by inducing proximity between a target protein and an usually unrelated protein of the disposal machinery, either of the ubiquitin-proteasome system (UPS) or the autophagy-lysosome system (ALS). Following the formation of a ternary complex, degradation of the target protein is initiated. The concept of targeted degradation shows several advantages over occupancy-driven target inhibition. In contrast to inhibitors, which require stoichiometric amounts of a drug, are degraders able to work in a catalytic manner, meaning sub-stoichiometric doses are sufficient. This is not only beneficial in terms of toxicity and side effects, also problems regarding drug resistance due to impaired inhibitor binding could be overcome. Furthermore, the requirements regarding binding affinity of degraders are relaxed compared to inhibitors and the binding site of the degrader does not play an important role. This aspect opens the door to target previously 'undruggable' proteins exhibiting shallow pockets and smooth surfaces which are unavailable for inhibitors.[1][2]

2.2 Ubiquitin-Proteasome System

The majority of the intracellular proteins are degraded *via* the ubiquitin-proteasome system. In this process, protein substrates are post-translational modified with the protein ubiquitin. By covalently attaching a polyubiquitin chain, the protein substrate is marked for degradation *via* the proteasome. Ubiquitylation of the proteins is a cascade process with three important enzymes involved. First, ubiquitin is activated in an ATP dependant manner, catalyzed by the ubiquitin activating enzyme E1. In this step, a thioester

bond is formed between the C-terminus of ubiquitin and a cysteine residue of the E1 enzyme. Subsequently, ubiquitin is transferred from E1s cysteine residue to an E2 cysteine residue, mediated by the E2 conjugating enzyme. Then, the E3 ubiquitin ligase mediates the transfer of ubiquitin from the E2 enzyme onto the protein substrate. E3 ligases act as bridging factors that enable close proximity of the E2 enzyme and the substrate protein. After the addition of the first ubiquitin to the protein substrate, the above described conjugation cascade is repeated, leading to the formation of a polyubiquitin chain, where ubiquitin molecules are linked via isopeptide bonds.[2][3]

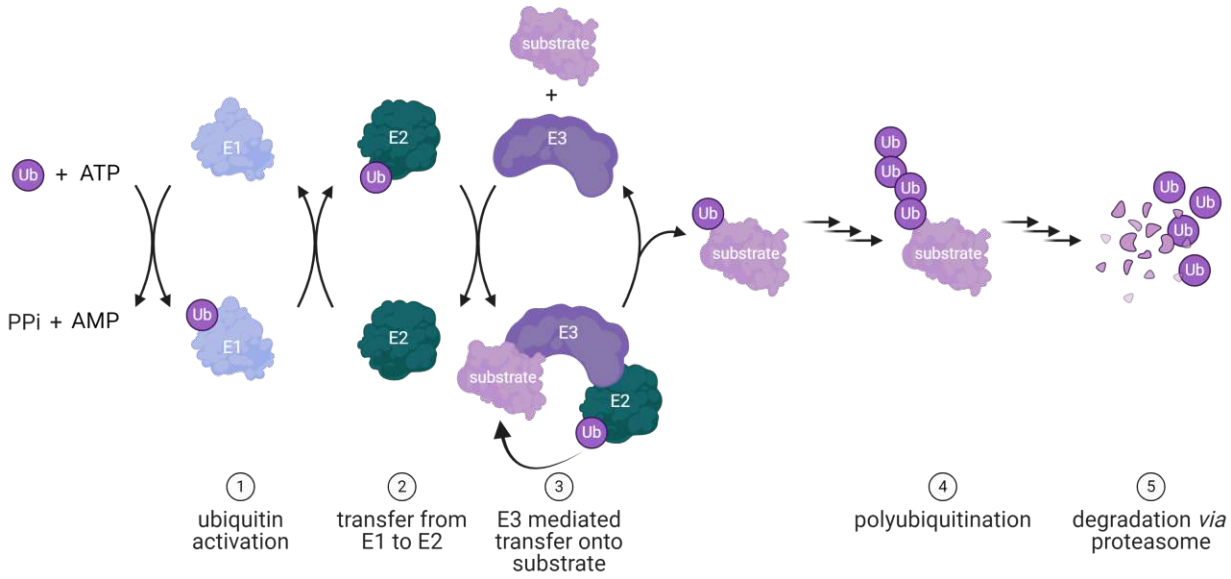

Figure 2.1: Illustration of the ubiquitylation process.

2.3 Strategies in TPD

Small molecule degraders are commonly classified regarding their mode of action either as monovalent or bivalent degraders. Bivalent degraders are heterobifunctional molecules that consist of two binding ligands connected by a linker. One of the ligands binds to the disposal machinery protein, the other one binds to the target protein. If both ligands are bound to their protein, the close proximity required for ubiquitination is provided and degradation can follow. Due to their structure, bivalent degraders are susceptible to rational design which is a huge advantage. In principle, only ligands for the E3 ligase as well as for the target protein are required. Then it is a matter of optimization, adjusting linker length and composition and determining the best exit vector for the ligand, to realize the bivalent degrader. These days, the diversity of bivalent degraders is high, from the most prominent representatives, proteolysis targeting chimeras (PROTACs) of all kinds, to lysosome-targeting chimeras (LYTACs) and autophagy-targeting chimeras (AUTACs), to name but a few.[4][5][6] In the last years, the number of bivalent degraders

has tremendously increased, which can easily be demonstrated with the help of PROTAC-DB, an open-access data bank. When it was launched in 2020, 1662 PROTACs were registered there, by 2022 it was 3270 and today the database contains 6111 PROTACs.[7][8][9] However, the structure of bivalent degraders has disadvantages too, as their relatively high molecular weight makes it difficult to achieve the desired properties for oral delivery, metabolite-related toxicity and central-nervous system exposure.

Monovalent degraders, on the other hand, can be further divided in perturbage-type and molecular glue-type degraders. When acting as perturbagens, monovalent degraders initiate the target proteins formation of a susceptible conformation state that can be degraded. In the molecular glue case, the degrader binds either to the disposal or the target protein. Thus, the proteins surface is modified which enables the interaction with the other one. Monovalent degraders have a lower molecular weight in general and therefore better drug-like properties. Furthermore, they are considered superior in targeting proteins with smooth surfaces. Not even a ligand for the respective protein is required, only a site for covalent binding which is usually an electrophilic moiety. Besides showing decent advantages, rational design of monovalent degraders in a target-based manner is almost impossible. Most of the monovalent degraders known today have been discovered serendipitously, the best example being thalidomide which was found to degrade neo-substrates such as zinc-finger transcription factors *via* E3 ligase Cereblon (CRBN).[1][6]

2.4 Need for new E3 Ligases

However, for mono- as well as for bivalent degraders, it is the E3 ubiquitin ligase that determines substrate specificity. Each E3 ligase is specific for a distinct and restricted substrate group, which is reflected in their large number. Nevertheless, while more than 600 E3 ligases are encoded in the human genome, only about 1% of them have been explored in targeted protein degradation so far. When looking at small molecule degraders that are currently in clinical trials, almost all of them are based on E3 ligase Cereblon (CRBN). Additionally, a few degraders target E3 ligase von Hippel-Lindau (VHL), but besides those two, there are no promising degraders in clinical studies that use any of the hundreds of other E3 ligases.[10][11] As each E3 ligase is highly specific, it is considered a tremendous opportunity to exploit new E3 ligases with differentiated properties. Regarding their properties, ligases also show different expression profiles. While CRBN and VHL are ubiquitously expressed, are other ligases expressed in specific tissues and cells and some ligases are tumor enriched or even tumor dependant. Furthermore, especially in oncology, there are concerns about resistance, meaning that tumor cells might mutate to evade degraders that are based on non-essential ligases such as CRBN and VHL. And last but not least, it has to be noted that most described degraders focus on oncology, however, by exploiting new E3 ligases it could be possible to target proteins that are related to areas such as inflammation, auto-immune diseases, viral infections or neurology.[11]

2.5 MMH1

Recently, Li *et al.* described a new covalent degrader, termed MMH1 (see Figure 3.1 A). The core of this small molecule degrader consists of JQ1, which is a known inhibitor of bromodomain-containing protein 4 (BRD4). BRD4, as a member of the bromodomain and extra-terminal domain (BET) protein family, is involved in immune response accompanying cancer cell growth. Inhibition of BRD4 by JQ1, however, was found to reduce cancer cell viability, as it leads to cell cycle arrest and promotes apoptosis of tumor cells. However, in MMH1 the chlorine of JQ1 is substituted with an acrylamide moiety. Due to this additional moiety, MMH1 does not inhibit, but degrades BRD4. Upon investigation of MMH1s mode of action, Li *et al.* found that it forms a ternary complex with BRD4 and E3 ligase receptor DCAF16, resulting in BRD4 ubiquitination and proteasome mediated degradation, respectively. More precisely, they found that the JQ1 moiety interacts with BRD4 and only like this, the acrylamide is aligned just in the right way to covalently bind to a cysteine (Cys58) of DCAF16. Like this, MMH1 stabilizes the weak native interaction of BRD4 and DCAF16 and enables BRD4 degradation.[12][13][14]

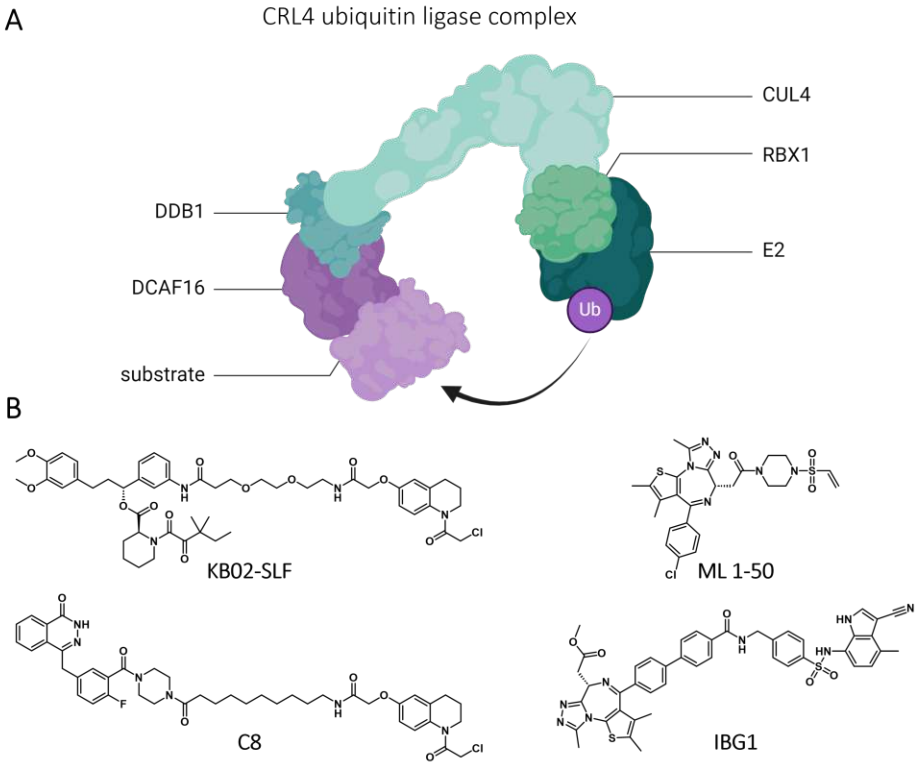

Figure 2.2: (A) Illustration of CRL4 ubiquitin ligase complex. (B) Selection of degraders working *via* DCAF16.

2.6 DCAF16

DCAF16, short for DDB1 (DNA-damage binding protein 1) and CUL4 (Cullin ubiquitin ligase 4) associated factor 16, belongs to the the DCAF protein family that counts more than hundred members. They act as substrate receptors of CRL4 (Cullin-RING ligase) ubiquitin ligase complexes and thus, mediate ubiquitination of substrate proteins, see Figure 2.2 A for an illustration of such a complex. DCAF16 is exclusively located in the nucleus, which can be exploited in terms of specificity to degrade nuclear proteins only while sparing cytosolic proteins.[15][16] Some degraders that function *via* DCAF16 are already described in the literature. Examples include PROTACs KB02-SLF from Zhang *et al.* and C8 from Pu *et al.*, monovalent degrader ML 1-50 from the Nomura lab or bivalent glue IBG1 from a recent patent, which was found to interact with DCAF16 by Hsia *et al.* Still, DCAF16 remains a poorly characterized E3 ligase receptor protein. In order to develop future degrader drugs based on DCAF16, it is required to gain more knowledge about this certainly interesting protein and find new compounds that interact with it.[16][17][18][19][20]

2.7 Aim

The aim of this thesis is the development of an assay to find new covalent binders of E3 ubiquitin ligase DCAF16. In this regard, two derivatives of the literature known covalent degrader MMH1 that carry a biotin moiety should be synthesized. The idea is to use these derivatives as probes that compete with new potential binders in the assay. The presence of the biotin moiety would allow streptavidin mediated visualization and pulldown of the formed complex with DCAF16. Figure 2.3 shows an outline of the envisioned assay.

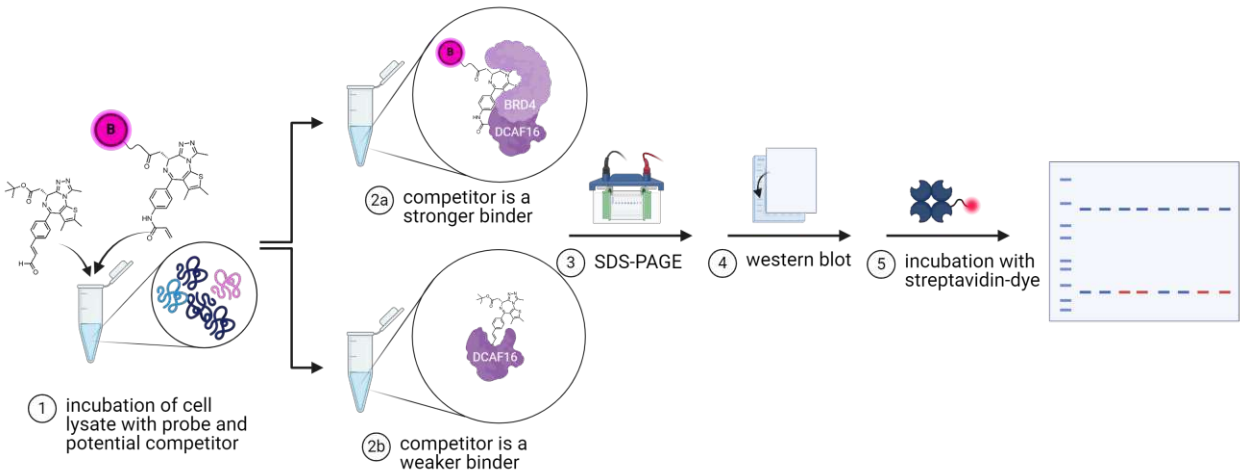

Figure 2.3: Outline of the envisioned assay.

Chapter 3

Results and Discussion

3.1 Approach

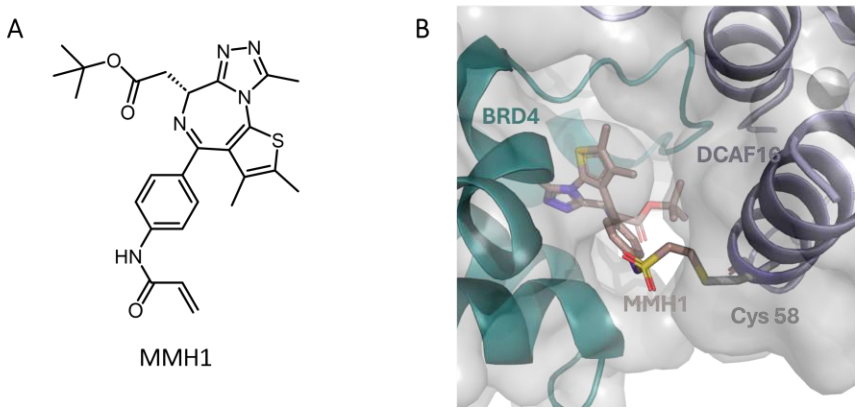

Figure 3.1: (A) Structure of **MMH1**. (B) **MMH1** covalently bound to DCAF16 while interacting with BRD4.

Regarding recently described degrader **MMH1**, not only its interaction with BRD4 and DCAF16 is known, Li *et al.* also created a three dimensional model of the respective interaction, which can be accessed *via* the Protein Data Bank (PDB: 8G46).[12] Figure 3.1 shows the structure of **MMH1** as well as **MMH1** interacting with BRD4 and DCAF16, to the latter one covalently bound.

When studying the orientation of **MMH1** between the two proteins, it was surmised that the installation of an exit vector should be possible either on the *tert*-butyl site or on the acrylamides' nitrogen of **MMH1**. This hypothesis is supported by known BRD4 degraders such as **KB02-JQ1** from Zhang *et al.* or **IBG1** from Hsia *et al.* These compounds are modified on the above-mentioned positions (see Figure 2.2 B) and degrade BRD4 *via* DCAF16.[16][20] Following this rationale, two probes **B1** and **B2** were designed. Both of the compounds carry a biotin functionality, **B1** on the *tert*-butyl site, **B2** on the acrylamide site of **MMH1**, as shown in Figure 3.2.

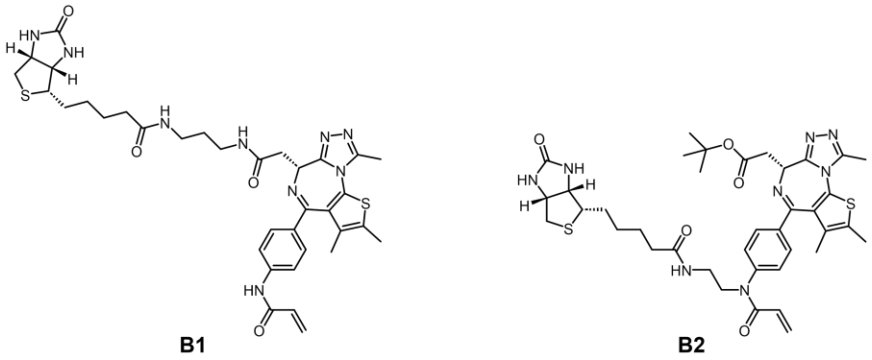

Figure 3.2: Structures of the designed probes **B1** and **B2**.

3.2 Synthesis

3.2.1 MMH1

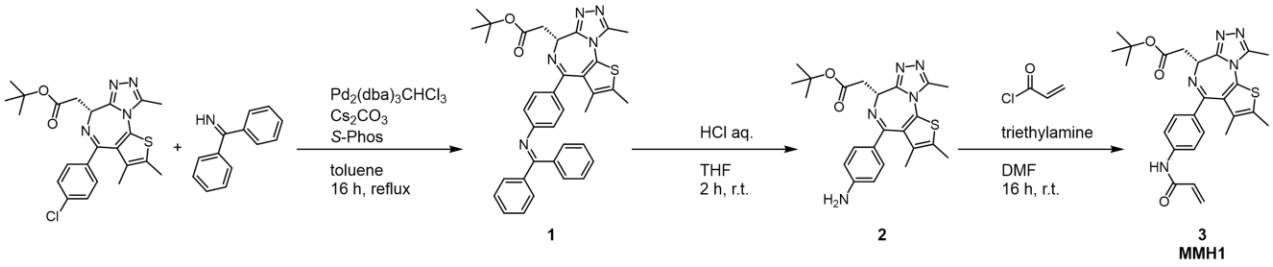

Scheme 3.1: Synthesis route of **MMH1**.

First, the literature known compound **MMH1** was synthesized. Scheme 3.1 shows its respective synthesis route, which started from commercially available (+)-JQ1. In the first step, a Buchwald-Hartwing coupling was performed to couple diphenylmethanimine to (+)-JQ1. In this coupling, $Pd_2(dba)_3{\cdot}CHCl_3$ was used as catalyst, in combination with *S*-Phos as ligand and Cs_2CO_3 as base. With a yield of 72% the Buchwald-Hartwig coupling was considered successful.

The coupling afforded compound **1**, which was deprotected next by applying hydrochloric acid in THF. Subsequently, the resulting product, compound **2**, was converted into an acrylamide *via* a nucleophilic substitution with acryloyl chloride. After this three steps, **MMH1** was obtained as a yellow solid.

3.2.2 B1

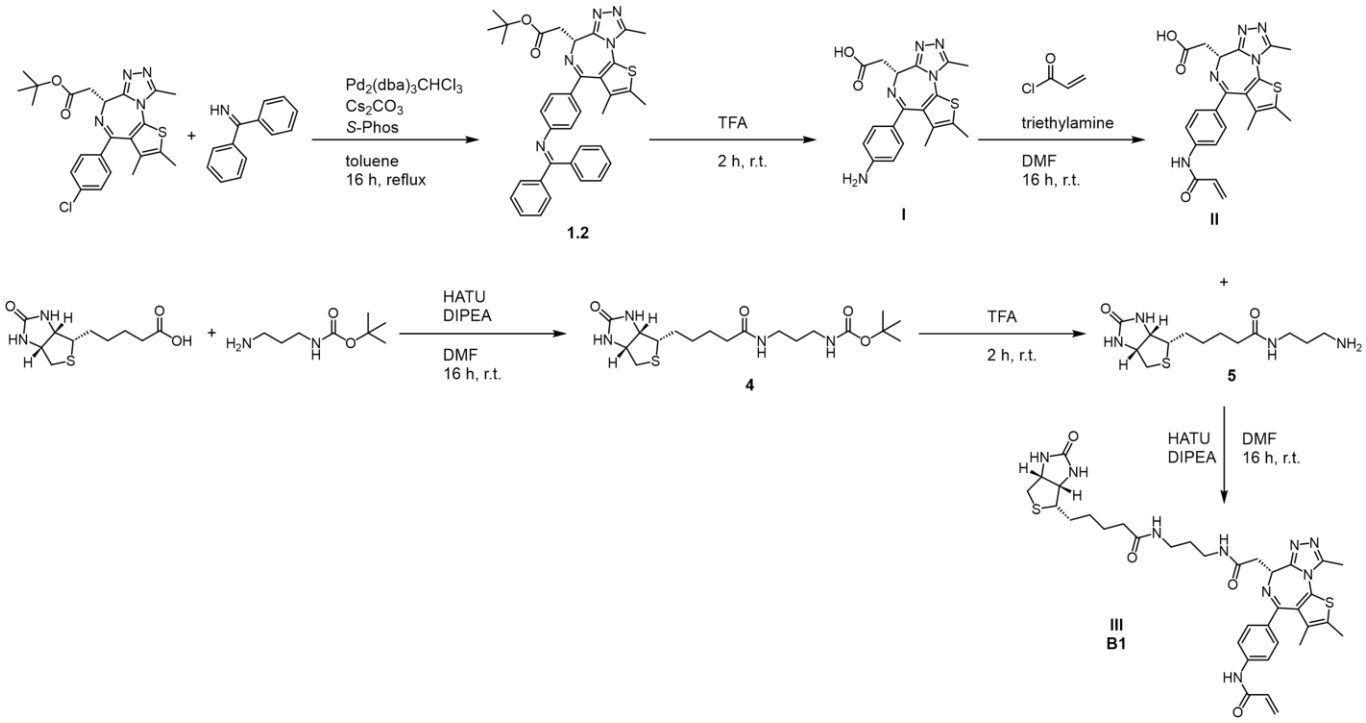

Scheme 3.2: Synthesis route of **B1**.

Next, probe **B1** was synthesized following the route depicted in Scheme 3.2. Same as with **MMH1**, the synthesis of **B1** started with the Buchwald-Hartwig coupling of (+)-JQ1 and diphenylmethanimine followed by a deprotection. In order to remove the *tert*-butyl group as well, the deprotection was carried out under harsher conditions compared to **MMH1**. This yielded compound **I**, which subsequently was converted into the acrylamide carrying compound **II** *via* a nucleophilic substitution with acryloyl chloride.

For the installation of biotin, an amide coupling with biotin linked to an amine was envisioned. However, the biotin-amine **5** had to be synthesized first. Starting from D-(+)-biotin, an amide coupling with *tert*-butyl (3-aminopropyl)carbamate using HATU as coupling reagent was performed. After the coupling the Boc-protecting group was removed by applying TFA affording compound **5**. Besides the product signals, ^{1}H NMR and ^{13}C NMR showed only traces of HATU impurities. Thus, the crude product was used without further purification in the next step, which consisted of another HATU coupling. After this final coupling of biotin-amine **5** with compound **II**, probe **B1** was obtained as a yellow solid.

3.2.3 B2

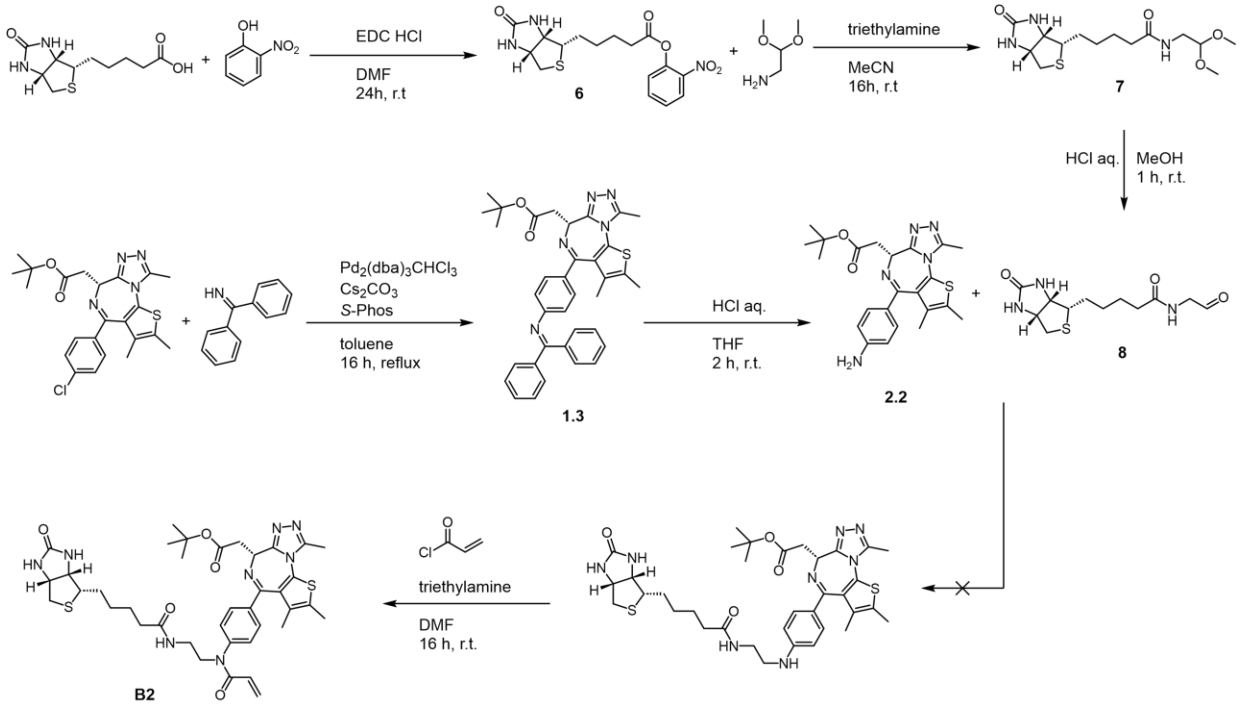

Scheme 3.3: Synthesis route of **B2**.

The first two steps in the synthesis of probe **B2** were exactly the same as for **MMH1**, leading to the successful synthesis of compound **2.2**. Next, a reductive amination with biotin-aldehyde **8** was envisioned. However, starting from D-(+)-biotin, compound **8** had to be synthesized first. The first step consisted of an EDC mediated coupling with 2-nitrophenol to activate the carboxylic acid. Subsequently, a nucleophilic substitution with 2,2-dimethoxyethan-1-amine was performed, converting the activated carboxylic acid into an amide, namely compound **7**.

Compound **7** represents the acetal-protected version of the desired biotin-aldehyde. Deprotection of the acetal was carried out by a solution of aqueous HCl and methanol, to yield free aldehyde **8**. The respective deprotection was performed right before the reductive amination was set up. This deprotection reaction is known to be very fast and indeed, after 1 h full conversion of the starting material was observed *via* LC-MS. Thus, the solvent was removed and the crude aldehyde **8** was directly used in the reductive amination.

In a first attempt, the reductive amination was carried out following a procedure from Ke *et al.* using $NaB(OAc)_3H$ as reducing agent in a MeOH/DCM (5/30) mixture with a catalytic amount of acetic acid.[21] With these conditions, only a minimal amount of product formation was observed by LC-MS after 2 h. However, even after a total of 24 h and the addition of another equivalent of reducing agent, product formation was not significantly increased.

According to Abdel-Magid and Mehrmann, using MeOH and DCM as solvents in combination with $NaBH(OAc)_3$ as reducing agent was not ideal. In presence of MeOH, the reduction of the carbonyl group is in competition with the reduction of the imine intermediate, especially when aldehydes are used. Additionally, DCM should be avoided as solvent, due to its tendency to react with amines. Therefore, the solvent of choice for reductive aminations with $NaBH(OAc)_3$ is DCE, yet also other polar aprotic solvents such as THF, acetonitrile or DMF work fine. Furthermore, if the reacting species is an aldehyde, addition of acid can be counterproductive, because it can favor the aldehydes reduction.[22]

Therefore, after the deprotection of compound **7** different solvents for performing the reductive amination step were screened. Among the polar aprotic solvents, THF could not be used due to insolubility of the reactants, so DMF was chosen as solvent. However, after 2 h only about 5% of product was observed and the addition of an extra equivalent of $NaBH(OAc)_3$ did not help the conversion of the starting material, even after another 3 h of stirring at room temperature.

The reducing agent chosen, $NaBH(OAc)_3$, is a very selective, yet mild agent. In combination with the amine being weakly basic and a weak nucleophile, aldehyde reduction was probably favored over reductive amination.[22] Therefore, instead of using $NaBH(OAc)_3$, the amination was tried with $NaBH_4$ as reducing agent. The protocol followed used $NaBH_4$ in combination with TMSCl as activating agent and DMF as solvent. The authors of the method, Pletz *et al.*, claim, that using this conditions, the reductive amination will proceed within minutes at 0 °C, even for electron-deficient aromatic amines.[23] Nevertheless, after 20 min only little product formation could be observed. Even after 24 h and the addition of another equivalent of $NaBH_4$, there was no increase in product formation. Although the authors describe the chosen conditions as very selective and without a great extend of carbonyl reduction, it is considered most likely that aldehyde **8** was reduced. In this regard, it has to be noted that Pletz *et al.* mainly examined ketones and only three highly electrophilic aldehyde substrates.

In a last attempt, $NaBH_3CN$, another very common reducing agent, was used for the reductive amination. A major advantage of $NaBH_3CN$ is its stability in acidic solutions as well as its solubility in hydroxylic solvents, for example in MeOH. Furthermore, $NaBH_3CN$ offers different selectivities based on the pH value. At neutral to weakly acidic pH, imines or iminium ions are reduced faster compared to carbonyl groups, whereas at pH 3-4, ketones and aldehydes are readily reduced.[22] Thus, the reaction was carried out at neutral pH. Nonetheless, also with this conditions, the reductive amination could not be achieved. Besides a trace of product, LC-MS showed that the starting material **2.2** was left while the aldehyde **8** was reduced. In summary, the reductive amination of JQ1-derivative **2.2** and aldehyde **8** could not be realized. An overview of the conditions that were tested can be found in Table 3.1.

Table 3.1: Conditions used for the reductive amination of amine **2.2** and aldehyde **8**.

reducing agent	additive	solvent
1.2 eq. $NaBH(OAc)_3$	cat. AcOH	MeOH/DCM (5/30)
1.4 eq. $NaBH(OAc)_3$	-	THF
1.4 eq. $NaBH(OAc)_3$	-	DMF
1.0 eq. $NaBH_4$	2.5 eq. TMSCl	DMF
1.8 eq. $NaBH_3CN$	-	MeOH

3.3 Confirmation Mode of Action B1

In the meantime, probe **B1** was analyzed regarding its mode of action *in vivo*. In order to use **B1** as a probe for the assay, it was essential to confirm that the compound interacts with DCAF16. As **B1** features, apart from its additional biotin-moiety, the same structure as **MMH1**, it should, same as **MMH1**, degrade BRD4 *via* DCAF16. Provided that **B1**s additional biotin-moiety does not interfere with the protein-protein interaction.

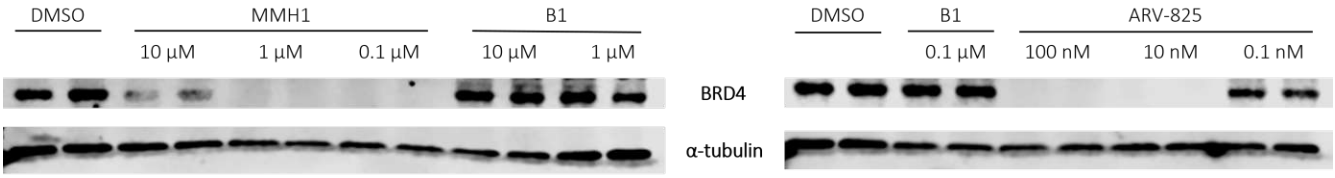

Figure 3.3: Western blots showing that envisioned probe **B1** is not able to degrade BRD4, while positive controls **MMH1** and **ARV-825** degrade BRD4 as described in the literature.

Therefore, the dose-dependant BRD4 degradation by **B1** was studied in HeLa cells, the respective western blot can be seen in Figure 3.3. However, at the concentrations studied, 10 µM, 1 µM and 0.1 µM, **B1** was not able to effectively degrade BRD4. **MMH1**, on the other hand, that served as a positive control, degraded BRD4 as described in the literature.[12] In this experiment, also PROTAC **ARV-825** was included as a positive control. **ARV-825** is a well studied PROTAC that degrades BRD4 *via* E3 ligase CRBN, not DCAF16. This compound is known to degrade at nanomolar concentrations which could be confirmed here as well.[24]

One possible reason why **B1** failed to degrade BRD4 could be a low cell membrane permeability of the compound. Therefore, the experiment was repeated, but in presence of lipofectamine. This is a common transfection reagent which can not only be used to deliver genetic material, but can also be used to improve the uptake of small molecules. However, even in presence of lipofectamine, **B1** was not able to degrade BRD4 in HeLa cells as shown in Figure 3.4.

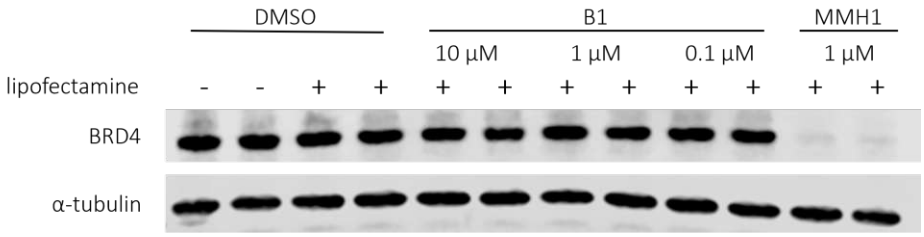

Figure 3.4: Western blot showing that even with lipofectamine added, **B1** is not able to degrade BRD4.

Together, these experiments show that the presence of the additional biotin moiety at the *tert*-butyl site of **MMH1** disturbs the interaction of BRD4 and DCAF16. As **B1** does not act as a degrader of BRD4, binding of **B1** to DCAF16 can not be confirmed. Therefore, it is not possible to use compound **B1** as a probe for the assay.

3.4 New Strategy

As discussed above, it was not possible to confirm the interaction of **B1** with DCAF16 because no BRD4 degradation could be observed. Considering the results discussed above, it was decided to change the strategy.

The idea of the new strategy was to replace the biotin moiety of **B1** at the *tert*-butyl site with an alkyne handle. The alkyne handle is much smaller than the biotin moiety and thus, might not disturb the interaction of the two proteins. Additionally, having an alkyne is tremendously advantageous because it allows the introduction of various other functionalities *via* a copper-catalyzed azide–alkyne cycloaddition (CuAAC) reaction. For example, biotin can be introduced *via* CuAAC, allowing to conduct the same experiment as envisioned and also biotin mediated pulldown experiments. Furthermore, also a fluorophore can be installed, enabling a direct confirmation of the binding event.

3.5 Synthesis of A1

The synthesis of the new, clickable probe **A1** was very similar to the synthesis of probe **B1**, see Scheme 3.4. Starting from (+)-JQ1 a Buchwald-Hartwig coupling and deprotection of the Boc-group followed by a nucleophilic substitution with acryloyl chloride afforded compound **II.2**. Afterwards, HOBt mediated coupling with propargyl amine led to the formation of the desired compound **A1**.

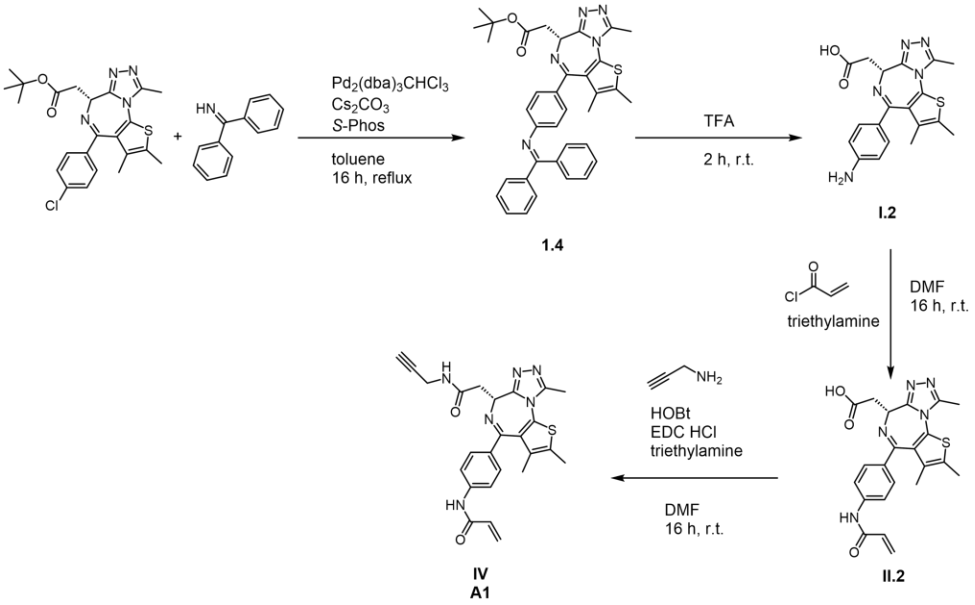

Scheme 3.4: Synthesis route of **A1**.

3.6 Degradation Activity A1

Following the successful synthesis of **A1**, the next step was to check if the compound not disturbs but interacts with DCAF16, leading to BRD4 degradation. Therefore, same as with **B1**, it was investigated whether **A1** degrades BRD4 or not. Again, HeLa cells were treated for 24 h with concentrations of 10 µM, 1 µM and 0.1 µM of **A1** and a western blot was done. In contrast to **B1**, the results of the **A1** treatment looked promising. At concentrations of 10 µM and 1 µM, partial degradation of BRD4 was observed (Figure 3.5). This leads to the conclusion that **A1** interacts with DCAF16 and can be used as a probe in the competition assay.

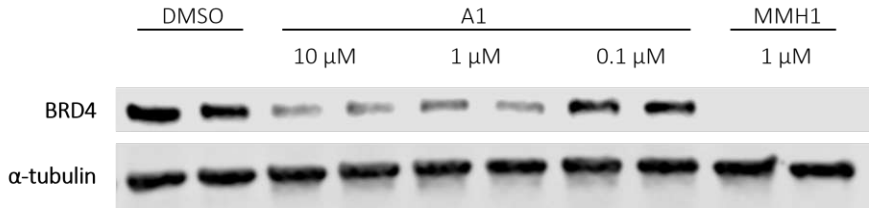

Figure 3.5: Western blot showing BRD4 degradation upon treatment with **A1**.

3.7 Fluorescent Labeling of DCAF16

Due to the promising results of the degradation study, next, it was investigaed if a fluorescent labeling of DCAF16 could be achieved. Therefore, HeLa cell lysates were incubated with 1 µM **A1** and afterwards clicked in a CuAAC with cyanine5.5-azide, which is a widely used fluorescent dye. Some samples were treated with DMSO only or **MMH1** to have negative controls. Additionally, lysates were also treated at the same time with **A1** and **MMH1**, to potentially see a competition leading to a fainter band. When imaging the gel, a fluorescent band at the molecular weight of DCAF16, at 24 kDa, was expected for all samples to which **A1** was added. However, no fluorescent bands could be observed (see Figure 3.6 A).

A possible reason for this unexpected result could have been that DCAF16 and / or BRD4 were damaged during cell lysis with RIPA buffer, which are considered harsh lysis conditions. If this was the case, the interaction of **A1** might have been disturbed. To test whether this was the case, not cell lysates but living cells were treated with **A1**, **MMH1** and DMSO. The treatment was performed for 6 h at concentrations of 10 µM of **A1** or **MMH1**. The treatment time was set at 6 h, as no (complete) degradation of BRD4 was expected after this time, but an interaction of the compounds with DCAF16. Afterwards, cells were lysed and the normalized lysates were clicked with CY5-azide. Nonetheless, the resulting gel looked exactly as the gel of the lysate - no fluorescent bands were observed, see Figure 3.6 B.

In conclusion, performing a CuAAC of cyanine5.5-azide with cell lysates or cells that were treated with **A1** and thus, labeling DCAF16 could not be accomplished.

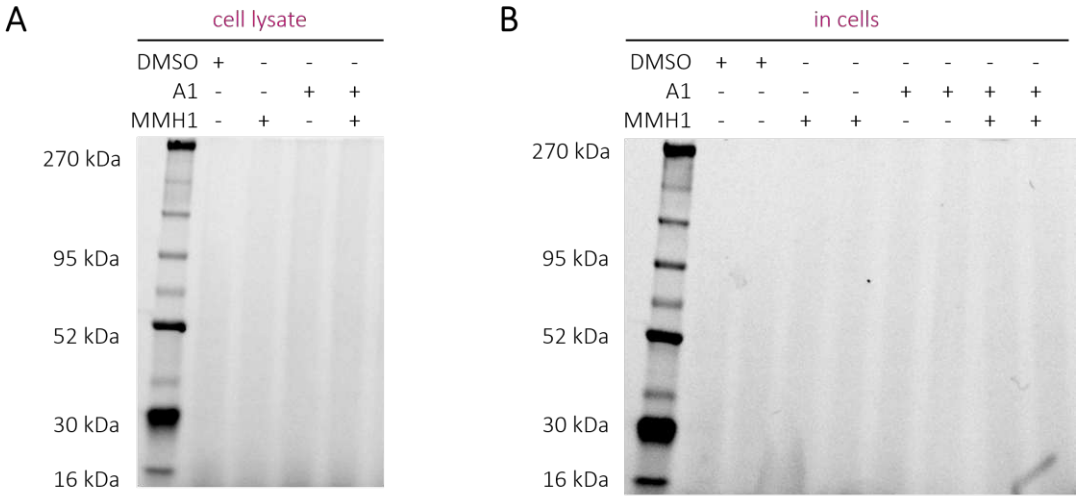

Figure 3.6: Upon treatment of cell lysate (A) and cells (B) with **A1** and subsequent CuAAC with CY5-azide, no fluorescent labeling of DCAF16 could be observed.

3.8 Optimization Click Conditions

Because prior results suggested that **A1** interacts with DCAF16, the fundamental aspect to test was whether the click reaction itself works or not. Hence, the CuAAC reaction was repeated under the conditions that were previously used, yet without lysate. Following the same procedure, **A1** diluted in RIPA buffer was mixed with the reagents of the CuAAC and after 2 h the samples were analyzed by UHPLC-MS. In addition to the large excess of CY5-azide, the analysis revealed only traces of the click product formed and a large amount of unreacted **A1**.

Therefore, the click conditions had to be optimized. Following the same protocol as before, new samples containing varying amounts of **A1** and CY5-azide in RIPA buffer without cell lysate were prepared. Furthermore, also a different protocol from BroadPharm, which uses higher concentrations of all reagents in general, was examined. The conditions studied are summarized in Table 3.2.[25]

Table 3.2: Conditions studied to optimize the CuAAC.

conditions	**A1** [µM]	**CY5-N_3** [µM]	**THPTA** [mM]	**$CuSO_4$** [mM]	**Na-asc.** [mM]	**time** [h]	outcome
original	1	25	1.25	0.25	5	2	only traces of click product
modified original	25	25	1.25	0.25	5	2	click reaction incomplete
	25	50	1.25	0.25	5	2	
	25	100	1.25	0.25	5	2	
	25	250	1.25	0.25	5	2	
new	25	250	5	1	15	0.5	complete conversion of A1
	25	250	5	1	15	1	
	25	250	5	1	15	2	

As shown in Table 3.2, only the conditions of BroadPharms protocol showed a complete conversion of **A1** and this even after 30 min of reaction. Therefore, these conditions, yet left for 2 h were used for further experiments.

3.9 Fluorescent Labeling New Conditions

With the optimized click conditions in hand, they were first applied to label DCAF16 in cell lysates. Thus, aliquots of fresh HeLa cell lysates were prepared and incubated with compound **A1** at 25 µM. Afterwards, the click reaction was performed using the optimized conditions, followed by separation of the samples by SDS-PAGE. When imaging the respective gel (see Figure 3.7), a fluorescent band at the molecular weight of DCAF16 was found.

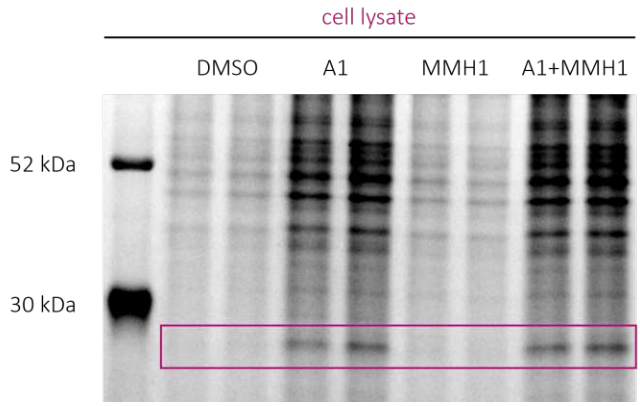

Figure 3.7: Gel of cell lysates that were treated with **A1** and later on clicked to CY5-azide using the optimized CuAAC conditions. The fluorescent bands at the molecular weight of DCAF16 are highlighted.

In addition to the cell lysate experiment, it was further investigated whether the labeling of DCAF16 could also be achieved *in vivo*. So far, it was not known with which concentrations cells have to be treated with **A1** so that a fluorescent labeling after cell lysis can be accomplished. Therefore, HeLa cells were treated with concentrations of **A1** ranging from 1 µM to 100 µM for either 6 h, 12 h or 24 h. Following the treatment, the cells were lysed and the CuAAC with CY5-azide was done using the optimized conditions. When treated with 100 µM **A1**, distinct bands at the molecular weight of DCAF16 could be observed for all treatment times, as well as faint bands when treated with 50 µM. Images of the gels after 6 h and 24 h can be found in Figure 3.8.

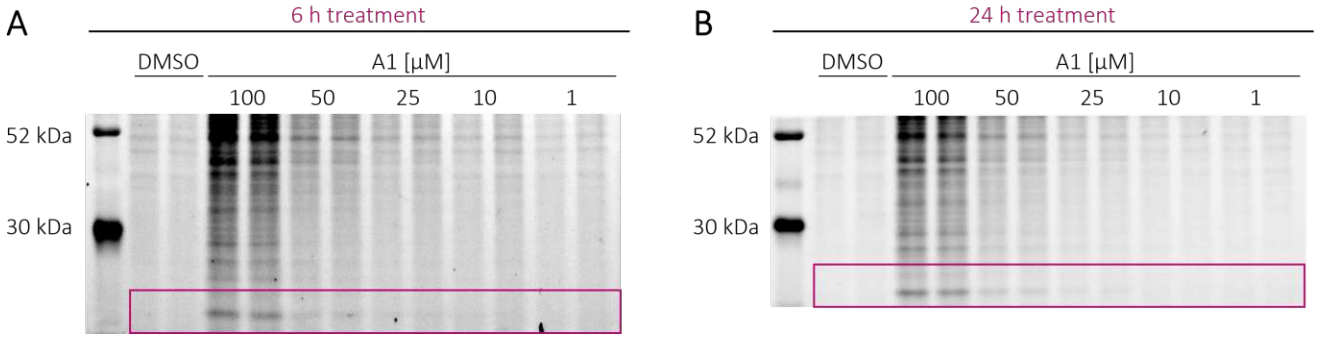

Figure 3.8: Resulting gels after treating HeLa cells with **A1** at concentrations from 1 µM to 100 µM for 6 h (A) or 24 h (B) and subsequent CuAAC with CY5-azide. The fluorescent bands corresponding to the molecular weight of DCAF16 are highlighted.

These results indicate that it is possible to covalently bind probe **A1** to DCAF16 and later on visualize the binding *via* CuAAC mediated click with a fluorophore. However, it has to be noted that the respective gels showed notable unspecific binding of probe **A1**. Therefore, it would be important to validate that **A1** truly binds to DCAF16 and hence, that the observed band really corresponds to DCAF16. This could be achieved by clicking not a fluorophore, but biotin and performing a pulldown of the labelled species with streptavidin beads followed by proteomics.

Chapter 4

Conclusion and Outlook

4.1 Conclusion

In order to develop an assay to find new covalent binders for E3 ligase DCAF16, two potential probes, **B1** and **B2**, were designed. The probes are based on **MMH1**, a known binder of DCAF16. However, in contrast to **MMH1**, **B1** and **B2** carry an additional biotin moiety that would allow streptavidin mediated fluorescent visualization and pulldown experiments. First, **B1** and **B2** had to be synthesized. While probe **B1** was successfully synthesized, a reductive amination step in the synthesis of **B2** has proven to be troublesome. Furthermore, also **MMH1** was successfully synthesized as a positive control. To confirm that the additional biotin moiety of **B1** does not disturb the interaction of **B1** with DCAF16 and BRD4, B1s ability to degrade BRD4 was studied. However, under the conditions studied, no degradation activity of **B1** could be observed. This leads to the conclusion that the implemented modification of **MMH1** hinders the interaction of **B1** with DCAF16 and BRD4. Therefore, **A1**, a new probe carrying a smaller, clickable alkyne at the *tert*-butyl site of **MMH1** was designed and successfully synthesized. Fortunately, **A1** was shown to degrade BRD4, confirming its possible application as a probe for the assay. Furthermore, the conditions of the CuAAC reaction to enable the addition of biotin or a fluorophore were optimized. Using the optimized CuAAC conditions, fluorescent visualization of DCAF16 in cell lysate and in cells, was succeeded upon treatment with **A1**.

4.2 Outlook

The very next step in order to finalize the setup of the assay would be a proof of concept experiment with **MMH1** as positive control. So far, **MMH1** was used at a concentration of 1 µM compared to **A1** at 25 µM. By using equal concentrations of both compounds, it can be assumed that **MMH1** occupies a significant amount of DCAF16, leading to a decreased or even absent fluorescent readout compared to incubation with **A1** only. Furthermore, it would be essential to perform a pulldown of the labeled protein followed by proteomics to verify DCAF16 as target of **A1**.

Once these prerequisites are confirmed, the assay is ready to be used. Subsequently, a structure-activity relationship (SAR) study of **MMH1** can be conducted and respective derivatives of **MMH1** can be studied regarding their ability to covalently bind to DCAF16 using the new assay. Promising candidates might then be further analyzed by global proteomics to investigate their mode of action.

Chapter 5

Experimental Part

5.1 Molecular Biology

5.1.1 Materials

Antibodies

The following antibodies were used: anti-BRD4 rabbit monoclonal antibody (abcam, ab128874, 1:500), anti-α-tubulin mouse monoclonal antibody (abcam, ab7291, 1:10000), anti-rabbit IgG secondary antibody (Licor, 926-32211 (800CW) and 926-68071 (680RD), 1:10000) and anti-Mouse IgG secondary antibody (Licor, 926-32210 (800CW) and 926-68072 (680RD), 1:10000). Furthermore, Streptavidin IRDye 680RD (Licor, 925-68079, 1:1000) was used.

5.1.2 Methods

Cell Culture

HeLa cells (ATCC) were cultured in high glucose DMEM (Sigma-Aldrich, D5796) with 10% fetal calf serum (BioConcept, 2-01F10-I) and 1% penicillin–streptomycin (BioConcept, 4-01F00-H) at 37 °C and 5% CO_2. Cells were passaged by trypsinization with 0.05% trypsin (Gibco, 25300054).

Immunoblotting

0.4 million HeLa cells were plated in 12-well plates containing 1 mL of media. After incubation overnight, cells were treated from DMSO stocks at indicated concentrations, whereas the final DMSO concentration was kept below 1%. After the indicated treatment times, cells were washed with PBS (BioConcept, 3-05F29-I), scraped and pelleted by centrifugation (8000 g, 10 minutes, 4 °C). Cell pellets were resuspended in RIPA lysis buffer (50 mM Tris at pH 8, 150 mM NaCl, 1% Triton X-100, 0.45% sodium deoxycholate, 0.1% SDS) supplemented with cOmplete Mini Protease Inhibitor (Roche) and 10 mM sodium orthovanadate (Sigma Aldrich) and left on ice for 30 min followed by centrifugation for 15 min at 21000 rcf and 4 °C. The supernatant was collected and protein concentration was measured using the DC-Protein Assay (BioRad). Aliquots of 20 µg protein were combined with 5X loading dye and denatured at 95 °C for 5 min while shaking at 300 rpm. Samples were then separated by SDS-PAGE applying 80-115 Volt and afterwards transferred onto nitrocellulose membranes using the Bio-Rad Trans-Blot Turbo Transfer system (Trans-Blot Turbo Mini 0.2 µm Nitrocellulose Transfer Packs 1704158, BioRad). Membranes were then blocked with Intercept (TBS) Blocking Buffer (LI-COR) for 1 h at r.t., incubated with primary antibody overnight, washed three times with TBST (5 min each wash) and incubated with secondary antibody for another 1 h at r.t.. Membranes were imaged using a LI-COR Odyssey XF imaging system and processed using LI-COR Empiria Studio Software.

Azide-Alkyne Click Chemistry

Protein concentration of the respective cell lysates were measured using the DC-Protein Assay. Then, aliquots of 18 µL with a protein concentration of 1.5 mg/mL in RIPA lysis buffer were prepared using amber eppendorf tubes. To these aliquots the following reagents were added: 3 µL of 2.5 mM Cyanine5-azide in DMSO (Lumiprobe, 33030), 3 µL of 10 mM $CuSO_4$ in water, 3 µL of 50 mM THPTA in water and 3 µL of 150 mM sodium ascorbate in water. The reaction mixture was pipetted to mix and then shaked at 25 °C for 2 h at 300 rpm. Afterwards, 5X loading dye was added, samples were denatured and analyzed by western blotting.

5.2 Chemistry

5.2.1 Materials

Reactants and Solvents

Chemicals and reagents were purchased from commercial vendors, including Sigma Aldrich, Acros, Alfa Aesar, Combi Blocks, Fisher Scientific, Biosolve, Flurochem and were used without further purification. Anhydrous solvents were purchased from Thermo Scientific, solvents used for preparative HPLC were purchased from VWR Chemicals and solvents for flash column chromatography from Biosolve Chemicals.

Unless otherwise noted, reactions were carried out under an nitrogen atmosphere in oven-dried glassware with magnetic stirring.

5.2.2 Methods

Chromatographic Analysis

Reaction monitoring was performed by thin layer chromatography using TLC alumina plates (Merck, silica gel 60, fluorescence indicator F254). For visualization, either UV light (254 nm) or heat staining of the plates with a ninhydrin solution was performed. Further reaction monitoring was performed by UHPLC on an Agilent 1290 Infinity system (ZORBAX Eclipse Plus RRHD, C18, 1.8 µm, 50 x 2.1 mm) equipped with an Agilent 6130 Quadrupole ESI-MS.

HR-MS measurements were performed on an Thermo Scientific Ultimate 3000 UPLC system combined with a Bruker maxis 4G ESI-Q-TOF mass spectrometer. The separations were performed on a reprospher 100 C18-Aqua 5 µm column (125 x 2 mm) at 30 °C with a flow rate of 0.5 mL/min and a water + 0.1% formic acid / acetonitrile + 0.1% formic acid gradient.

Chromatographic Purification

Flash column chromatography was performed using a Teledyne ISCO CombiFlash Rf+ system with either Biotage Sfär Silica D (Duo 60 µm) columns or cartridges packed with silica gel (Fisher Scientific, SilicaFlash P60 40-63 µm). Preparative HPLC was performed using a Shimadzu Prominence UFLC preparative liquid chromatography system with a Phenomenex Gemini column (5 µm NX-C18 110 Å, 250 x 21.2 mm).

NMR Spectroscopy

^{1}H and ^{13}C spectra were recorded either on a Bruker Avance III 400 MHz spectrometer or on a Bruker Avance III 500 MHz spectrometer at room temperature. Chemical shifts (δ) are reported in parts per million (ppm) related to tetramethylsilane and calibrated to deuterated solvent residual peaks. The data is shown as follows: Chemical shift, multiplicity (s = singlet, d = doublet, t = triplet, q = quartet, quin = quintet, sext = sextet, m = multiplet, br = broad signal) and integration.

5.2.3 Synthesis

***tert*-butyl (*R*)-2-(4-(4-((diphenylmethylene)amino)phenyl)-2,3,9-trimethyl-6*H*-thieno[3,2-*f*][1,2,4]triazolo-[4,3-*a*][1,4]diazepin-6-yl)acetate (1)**

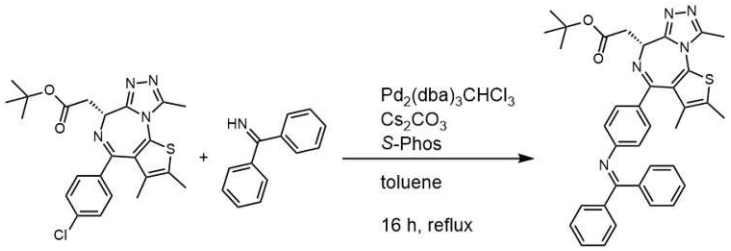

(+)-JQ1 (1 eq., 150.0 mg, 0.33 mmol) was dissolved in dry toluene (7.5 mL) under N_2 atmosphere, followed by addition of diphenylmethanimine (1.5 eq., 82.6 µL, 0.49 mmol), Cs_2CO_3 (3 eq., 320.8 mg, 0.98 mmol), $Pd(dba)_3 \cdot CHCl_3$ (0.1 eq., 34.0 mg, 0.03 mmol) and *S*-Phos (0.1 eq., 13.5 mg, 0.03 mmol). The dark suspension was heated to reflux for 15 h. Afterwards, the reaction was allowed to cool to r.t., filtered over Celite and the solvent was removed under reduced pressure. The brown residue was purified by column chromatography (10 g silica, CombiFlash Rf+, 0-100% ethyl acetate in cyclohexane). After removal of the solvent, the product **1** (162.7 mg, 82%) was obtained as an orange solid.

^{1}H NMR (400 MHz, DMSO-d_6) δ 7.71 – 7.64 (d, 2H), 7.61 – 7.39 (m, 3H), 7.32 – 7.25 (m, 3H), 7.17 (d, J = 8.0 Hz, 2H), 7.14 – 7.08 (m, 2H), 6.75 – 6.68 (m, 2H), 4.33 (t, J = 8.3, 6.2 Hz, 1H), 3.27 (dd, J = 9.9, 7.2 Hz, 2H), 2.58 (s, 3H), 2.39 (s, 3H), 1.49 (s, 3H), 1.40 (s, 9H) ppm.

^{13}C NMR (126 MHz, DMSO-d_6) δ 169.79, 168.19, 163.66, 154.97, 153.40, 132.51, 131.79, 131.20, 130.41, 130.09, 128.87, 128.75, 128.70, 128.43, 127.97, 120.16, 80.09, 69.87, 53.35, 37.46, 27.78, 13.69, 12.67, 11.22 ppm.

ESI-HRMS $[M+H]^+$ calcd. 602.26 for $C_{36}H_{36}N_5O_2S^+$, found 602.26.

***tert*-butyl *(R)*-2-(4-(4-aminophenyl)-2,3,9-trimethyl-6*H*-thieno[3,2-*f*][1,2,4]triazolo[4,3-*a*][1,4]diazepin-6-yl)acetate (2)**

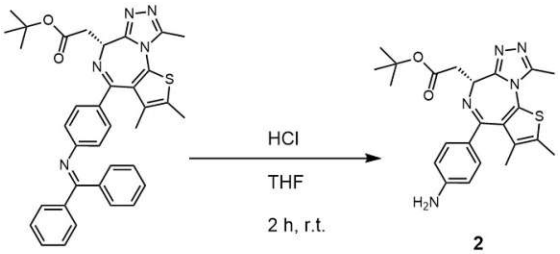

Compound **1** (1 eq., 135.0 mg, 0.22 mmol) was dissolved in THF (0.6 mL), followed by addition of 1M HCl (240 µL) in THF (0.6 mL) at 0 °C. The dark yellow solution was allowed to warm to r.t. and was stirred for 2 h until LC-MS showed full conversion. Then, the reaction was concentrated under reduced pressure to about 500 µL and was purified by column chromatography (4 g silica, CombiFlash Rf+, 0-10% MeOH in DCM). After removal of the solvent, the product **2** (43.7 mg, 45%) was obtained as an orange solid.

^{1}H NMR (500 MHz, DMSO-d_6) δ 7.22 (bs, 2H), 6.62 (d, J = 8.6 Hz, 2H), 4.60 (s, 1H), 3.36 (d, J = 7.5 Hz, 2H), 2.61 (s, 3H), 2.46 – 2.41 (m, 3H), 1.73 (d, J = 0.9 Hz, 3H), 1.43 (s, 9H) ppm.

^{13}C NMR (126 MHz, DMSO-d_6) δ 170.92, 167.41, 163.18, 156.90, 154.80, 142.69, 131.69, 131.27, 120.87, 113.38, 112.41, 105.45, 85.67, 59.47, 32.53, 27.75, 14.09, 12.79, 11.28 ppm.

ESI-HRMS $[M+H]^+$ calcd. 438.20 for $C_{23}H_{28}N_5O_2S^+$, found 438.20.

***tert*-butyl *(R)*-2-(4-(4-acrylamidophenyl)-2,3,9-trimethyl-6*H*-thieno[3,2-*f*][1,2,4]triazolo[4,3-*a*][1,4]diazepin-6-yl)acetate (3)**

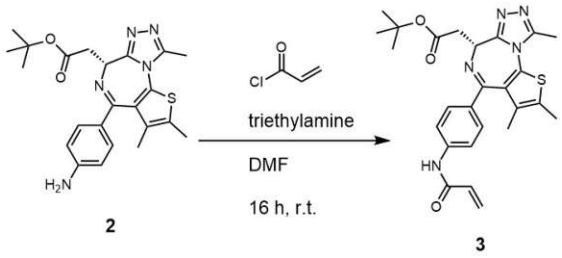

Compound **2** (1 eq., 42.0 mg, 0.10 mmol) was dissolved in dry DMF (0.9 mL) and triethylamine (3 eq., 40.1 µL, 0.29 mmol) was added. At 0 °C, acryloyl chloride (0.85 eq., 6.6 µL, 0.08 mmol) in dry DMF (100 µL) was added dropwise. The reaction was allowed to warm to r.t. and was stirred for 15 h under N_2 atmosphere. Then, the solvent was removed under reduced pressure and the crude product was purified *via* prep-HPLC (Gemini 5 µm NX-C18 110 Å, 250 x 21.2 mm, 1-99% MeCN + 0.1% TFA in H_2O + 0.1% TFA). After lyophilization, **3** (15.0 mg, 38%) was afforded as a yellow solid.

^{1}H NMR (500 MHz, DMSO-d_6) δ 10.35 (s, 1H), 7.71 (d, J = 9.0 Hz, 2H), 7.39 (d, J = 8.3 Hz, 2H), 6.44 (dd, J = 17.0, 10.2 Hz, 1H), 6.27 (dd, J = 16.9, 1.9 Hz, 1H), 5.78 (dd, J = 10.1, 1.9 Hz, 1H), 4.40 (dd, J = 8.2, 6.3 Hz, 1H), 3.39 – 3.25 (m, 2H), 2.60 (s, 3H), 2.42 (s, J = 0.9 Hz, 3H), 1.68 – 1.65 (s, 3H), 1.43 (s, 9H) ppm.

^{13}C NMR (126 MHz, DMSO-d_6) δ 169.75, 163.36, 156.55, 155.00, 149.79, 147.02, 141.14, 131.62, 130.71, 130.14, 129.12, 127.41, 118.79, 117.28, 105.27, 80.17, 53.37, 37.41, 27.79, 13.97, 12.70, 11.22 ppm.

ESI-HRMS $[M+H]^+$ calcd. 492.21 for $C_{26}H_{30}N_5O_3S^+$, found 492.21.

***(R)*-2-(4-(4-aminophenyl)-2,3,9-trimethyl-6*H*-thieno[3,2-*f*][1,2,4]triazolo[4,3-*a*][1,4]diazepin-6-yl)acetic acid (I)**

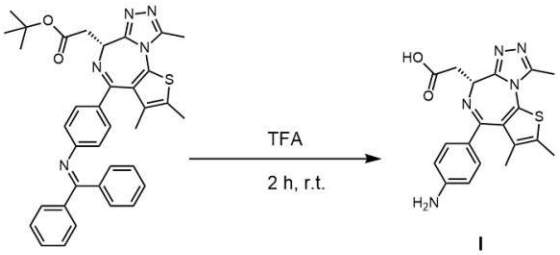

1 I

Compound **1** (1 eq., 100.0 mg, 0.17 mmol) was dissolved in DCM (1 mL) and at 0 °C TFA (1.6 mL) was added dropwise. The reaction as allowed to warm to r.t. and was stirred for 2 h until LC-MS showed full conversion. Again at 0 °C, water (10 mL) followed by DCM (10 mL) was added. The phases were separated and the organic phase was extracted with water (3 x 10 mL). The aqueous layers were combined, then water was removed under reduced pressure. The yellow residue was purified *via* prep-HPLC (Gemini 5 µm NX-C18 110 Å, 250 x 21.2 mm, 1-99% MeCN + 0.1% TFA in H_2O + 0.1% TFA). After lyophilization, compound **I** (54.5 mg, 86%) was obtained as a yellow solid.

^{1}H NMR (500 MHz, DMSO-d_6) δ 7.22 (s, 2H), 6.63 (d, 2H), 4.66 (s, 1H), 3.42 (dd, 2H), 2.62 (s, 3H), 2.45 (s, 3H), 1.74 (s, 3H) ppm.

^{13}C NMR (126 MHz, DMSO-d_6) δ 171.15, 167.22, 159.84, 158.53, 158.23, 154.69, 150.70, 142.14, 133.34, 131.84, 116.33, 113.50, 51.60, 33.86, 14.20, 12.83, 11.36 ppm.

ESI-HRMS $[M+H]^+$ calcd. 382.13 for $C_{19}H_{20}N_5O_2S^+$, found 382.13.

***(R)*-2-(4-(4-acrylamidophenyl)-2,3,9-trimethyl-6*H*-thieno[3,2-*f*][1,2,4]triazolo[4,3-*a*][1,4]diazepin-6-yl)-acetic acid (II)**

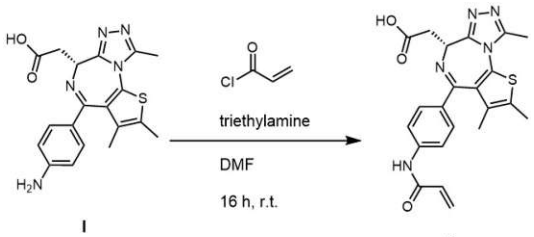

I II

Compound **I** (1 eq., 45.0 mg, 0.12 mmol) was dissolved in dry DMF (900 µL), then triethylamine (3 eq., 49.0 µL, 0.35 mmol) was added. At 0 °C, acryoyl chloride (0.85 eq., 8.2 µL, 0.10 mmol) dissolved in dry DMF (100 µL) was added dropwise. The turbid reaction mixture was allowed to warm to r.t. and was stirred under N_2 atmosphere for 16 h. Afterwards, the solvent was removed under reduced pressure and the yellow residue was purified by prep-HPLC (Gemini 5 µm NX-C18 110 Å, 250 x 21.2 mm, 1-99% MeCN + 0.1% TFA in H_2O + 0.1% TFA). After lyophilization, the product **II** (22.0 mg, 50%) was obtained as yellow solid.

^{1}H NMR (500 MHz, DMSO-d_6) δ 10.36 (s, 1H), 7.75 – 7.69 (d, 2H), 7.44 – 7.37 (d, 2H), 6.44 (dd, J = 17.0, 10.2 Hz, 1H), 6.27 (dd, J = 17.0, 1.9 Hz, 1H), 5.78 (dd, J = 10.1, 2.0 Hz, 1H), 4.45 (t, J = 7.1 Hz, 1H), 3.43 (dd, J = 16.7, 7.0 Hz, 1H), 3.31 (dd, J = 16.7, 7.3 Hz, 1H), 2.61 (s, 3H), 2.44 – 2.40 (s, 3H), 1.69 – 1.64 (s, 3H) ppm.

^{13}C NMR (126 MHz, DMSO-d_6) δ 171.99, 165.12, 163.36, 161.56, 158.04, 149.89, 141.21, 138.45, 137.97, 131.62, 130.76, 129.26, 127.42, 118.76, 117.38, 53.27, 36.45, 14.05, 12.71, 11.24 ppm.

ESI-HRMS $[M+H]^+$ calcd. 436.14 for $C_{22}H_{22}N_5O_3S^+$, found 436.14.

***tert*-butyl (3-(5-((3a*S*,4*S*,6a*R*)-2-oxohexahydro-1*H*-thieno[3,4-*d*]imidazol-4-yl)pentanamido)propyl)-carbamate (4)**

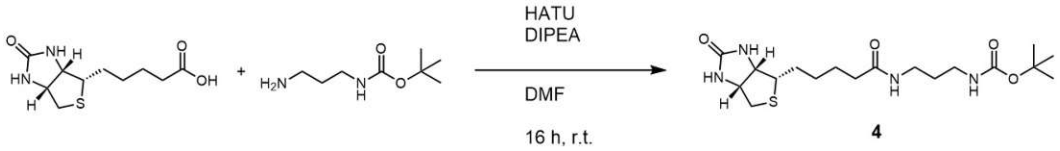

D-(+)-biotin (1 eq., 610 mg, 2.50 mmol), *tert*-butyl (3-aminopropyl)carbamate (1.5 eq., 653 mg, 3.75 mmol) and HATU (2 eq., 1.90 g, 5.00 mmol) were dissolved in dry DMF (70 mL), then DIPEA (5 eq., 2.2 mL, 12.5 mmol) was added dropwise. The reaction was stirred under N_2 atmosphere at r.t. for 16 h. Then, the reaction was concentrated *in vacuo*, followed by addition of ethyl acetate (100 mL). The organic phase was washed with water (3 x 70 mL) as well as brine (1 x 70 mL). The organic layer was dried over Na_2SO_4, filtered and the solvent was removed, yielding the crude product **4** (1.07 g) as a yellow solid. The crude compound **4** was used without further purification.

^{1}H NMR (500 MHz, DMSO-d_6) δ 7.73 (t, J = 5.7 Hz, 1H), 7.53 (dd, J = 8.7, 3.1 Hz, 1H), 6.42 (d, J = 1.8 Hz, 1H), 6.35 (s, 1H), 4.34 – 4.27 (m, 1H), 4.13 (ddd, J = 7.8, 4.4, 1.8 Hz, 1H), 3.12 – 2.96 (m, 5H), 2.82 (dd, J = 12.5, 5.1 Hz, 1H), 2.57 (d, J = 12.4 Hz, 1H), 2.04 (t, J = 7.4 Hz, 2H), 1.69 – 1.56 (m, 2H), 1.51 – 1.44 (m, 4H), 1.37 (s, 9H), 1.34 – 1.22 (m, 2H) ppm.

^{13}C NMR (126 MHz, DMSO-d_6) δ 171.99, 162.73, 151.11, 77.47, 61.04, 59.21, 55.40, 42.04, 39.45, 36.14, 35.24, 29.67, 28.26, 28.24, 28.04, 25.31 ppm.

ESI-HRMS $[M+Na]^+$ calcd. 423.20 for $C_{18}H_{32}N_4O_4SNa^+$, found 423.20.

***N*-(3-(2-*(R)*-4-(4-acrylamidophenyl)-2,3,9-trimethyl-6*H*-thieno[3,2-*f*][1,2,4]triazolo[4,3-*a*][1,4]diazepin-6-yl)acetamido)propyl)-5-((3a*S*,4*S*,6a*R*)-2-oxohexahydro-1*H*-thieno[3,4-*d*]imidazol-4-yl)pentanamide (III)**

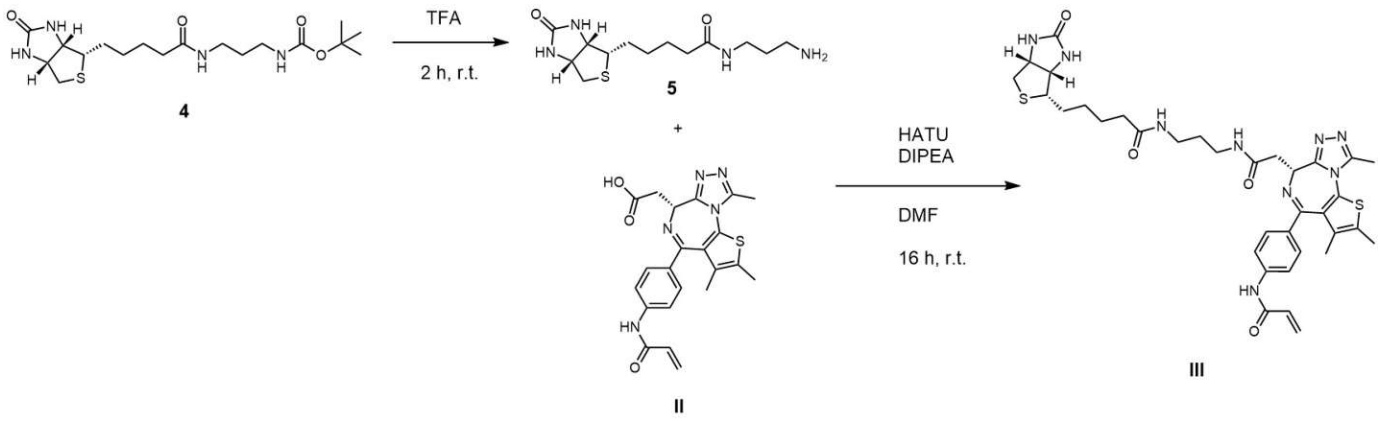

Compound **4** (1 eq., 100.0 mg, 0.25 mmol) was dissolved at 0 °C in TFA (20 eq., 382 µL, 5.0 mmol), then the yellow reaction was allowed to warm to r.t. and was stirred at r.t. for 2 h. Afterwards, the reaction was quenched at 0 °C with water (10 mL) and the aqueous phase was washed with DCM (2 x 10 mL). The solvent was removed under reduced pressure, leaving the crude intermediate **5** as a yellow oil (102 mg).

^{1}H NMR (500 MHz, DMSO-d_6) δ 7.81 (s, 1H), 6.42 (s, 2H), 4.31 (ddd, J = 7.8, 5.1, 1.0 Hz, 1H), 4.13 (dd, J = 7.8, 4.4 Hz, 1H), 3.18 (td, J = 7.3, 5.4 Hz, 2H), 3.14 – 3.06 (m, 3H), 2.82 (dd, J = 12.5, 5.1 Hz, 1H), 2.58 (d, J = 12.4 Hz, 1H), 2.08 (t, J = 7.4 Hz, 2H), 1.70 – 1.40 (m, 6H), 1.32 (dq, J = 20.0, 6.5 Hz, 2H) ppm.

^{13}C NMR (126 MHz, DMSO-d_6) δ 172.66, 162.75, 61.08, 59.24, 55.42, 41.60, 39.78, 36.82, 35.43, 28.25, 28.07, 27.55, 25.26 ppm.

ESI-HRMS $[M+H]^+$ calcd. 301.17 for $C_{13}H_{25}N_4O_2S^+$, found 301.17.

Compound **II** (1 eq., 17.0 mg, 0.04 mmol) was dissolved in dry DMF (1.5 mL), followed by addition of the crude intermediate **5** (1.5 eq., 17.6 mg, 0.06 mmol), HATU (2 eq., 29.7 mg, 0.08 mmol) and DIPEA (5 eq., 34 µL, 0.20 mmol). The light yellow solution was stirred at r.t. under N_2 atmosphere for 16 h. As LC-MS showed full conversion, the reaction was concentrated under reduced pressure. The residue was taken up with ethyl acetate (10 mL) and the organic phase was extracted with water (3 x 5 mL). The organic layer was dried over Na_2SO_4, then solvent was removed. The product was purified by prep-HPLC (Gemini 5 µm NX-C18 110 Å, 250 x 21.2 mm, 1-99% MeCN + 0.1% TFA in H_2O + 0.1% TFA). After lyophilization, compound **III** (11 mg, 40%) was afforded as a yellow solid.

^{1}H NMR (500 MHz, DMSO-d_6) δ 10.35 (s, 1H), 8.19 (t, J = 5.7 Hz, 1H), 7.75 (t, J = 5.7 Hz, 1H), 7.73 – 7.69 (m, 2H), 7.38 (d, J = 8.4 Hz, 2H), 6.44 (dd, J = 16.9, 10.2 Hz, 1H), 6.38 (s, 2H), 6.27 (dd, J = 17.0,

2.0 Hz, 1H), 5.78 (dd, J = 10.1, 2.0 Hz, 1H), 4.50 (dd, J = 7.8, 6.4 Hz, 1H), 4.28 (dd, J = 7.7, 5.0 Hz, 1H), 4.14 – 4.08 (m, 1H), 3.27 – 3.05 (m, 7H), 2.83 – 2.76 (m, 1H), 2.60 (s, 3H), 2.56 (d, J = 12.4 Hz, 1H), 2.42 (s, 3H), 2.06 (t, J = 7.4 Hz, 2H), 1.65 (s, 3H), 1.65 – 1.23 (m, 8H) ppm.

^{13}C NMR (126 MHz, DMSO-d_6) δ 171.97, 169.57, 163.40, 162.71, 158.91, 151.16, 148.92, 145.80, 138.67, 137.14, 133.24, 132.03, 129.29, 121.04, 116.98, 114.81, 90.48, 61.02, 59.20, 55.39, 53.49, 41.75, 40.68, 36.27, 35.29, 33.80, 28.02, 25.55, 24.70, 22.92, 14.05, 12.72, 11.26 ppm.

ESI-HRMS $[M+H]^+$ calcd. 718.30 for $C_{35}H_{44}N_9O_4S_2^+$, found 718.30.

***(R)*-*N*-(4-(2,3,9-trimethyl-6-(2-oxo-2-(prop-2-yn-1-ylamino)ethyl)-6*H*-thieno[3,2-*f*][1,2,4]triazolo[4,3-*a*][1,4]diazepin-4-yl)phenyl)acrylamide (IV)**

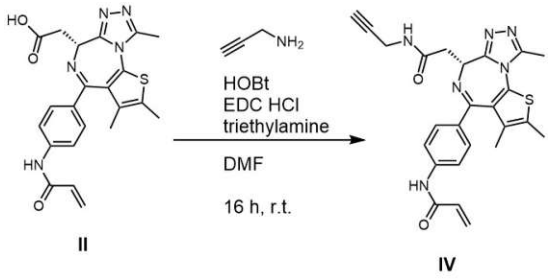

Compound **II** (1 eq., 9.4 mg, 0.02 mmol) was dissolved in dry DMF (1 mL), followed by addition of triethylamine (2.5 eq., 7.5 µL, 0.05 mmol) at 0 °C, turning the yellow solution clear. Still at 0 °C, EDC·HCl (1.5 eq., 6.2 mg, 0.03 mmol) followed by HOBt (1 eq., 3.3 mg, 0.02 mmol) was added. After 15 min of stirring at 0 °C, propargylamine (1.5 eq., 2.1 µL, 0.03 mmol) was added, then the clear solution was allowed to warm to r.t. and was further stirred for 16 h. As LC-MS showed complete conversion of the starting material, the solvent was removed *in vacuo* and the yellow residue was purified *via* prep-HPLC (Gemini 5 µm NX-C18 110 Å, 250 x 21.2 mm, 1-99% MeCN + 0.1% TFA in H_2O + 0.1% TFA). The product (9.3 mg, 91%) was obtained as yellow solid.

^{1}H NMR (500 MHz, DMSO-d_6) δ 10.34 (s, 1H), 8.67 (t, J = 5.5 Hz, 1H), 7.73 – 7.67 (m, 2H), 7.43 – 7.37 (m, 2H), 6.44 (dd, J = 16.9, 10.2 Hz, 1H), 6.27 (dd, J = 17.0, 2.0 Hz, 1H), 5.78 (dd, J = 10.1, 2.0 Hz, 1H), 4.50 (dd, J = 8.0, 6.2 Hz, 1H), 3.93 (qdd, J = 17.5, 5.5, 2.6 Hz, 2H), 3.31 – 3.17 (m, 2H), 3.14 (t, J = 2.5 Hz, 1H), 2.60 (s, 3H), 2.42 (d, J = 0.8 Hz, 3H), 1.65 (d, J = 0.9 Hz, 3H) ppm.

^{13}C NMR (126 MHz, DMSO-d_6) δ 170.33, 163.35, 161.36, 158.17, 154.02, 151.55, 147.09, 144.57, 141.09, 131.27, 130.64, 126.66, 121.94, 118.72, 115.56, 79.23, 72.59, 54.06, 37.08, 27.83, 14.05, 12.38, 11.25 ppm.

ESI-HRMS $[M+H]^+$ calcd. 473.18 for $C_{25}H_{25}N_6O_2S^+$, found 473.18.

2-nitrophenyl 5-((3a*S*,4*S*,6a*R*)-2-oxohexahydro-1*H*-thieno[3,4-*d*]imidazol-4-yl)pentanoate (6)

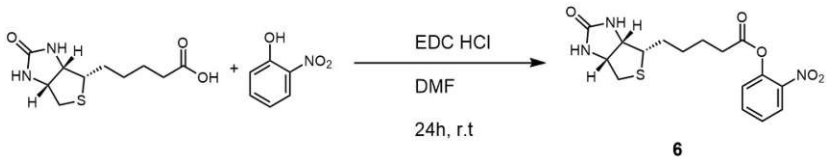

6

D-(+)-biotin (1 eq., 334 mg, 1.37 mmol) was suspended in dry DMF (7.0 mL), then EDC·HCl (1.2 eq., 315 mg, 1.64 mmol) was added and the white suspension was stirred at r.t. for 1 h. Afterwards, 2-nitrophenol (1.1 eq., 209 mg, 1.51 mmol) was added, turning the clear solution yellow. The reaction was further stirred at r.t. under N_2 atomsphere for 23 h. Then, the reaction was concentrated under reduced pressure to about 1/3 of the volume. While stirring, 1M HCl (15 mL) was added, leading to the formation of a white precipitate. The precipitate was filtered off and washed with 1M HCl (10 mL) as well as water (10 mL) and ethyl acetate (10 mL). The resulting white solid was dried under vacuum, then the crude was recrystallized in ethanol. After drying, compound **6** (107 mg, 21%) was obtained as a white solid.

^{1}H NMR (400 MHz, DMSO-d_6) δ 8.15 (d, J = 8.2 Hz, 1H), 7.83 (t, J = 7.9 Hz, 1H), 7.55 (t, J = 7.8 Hz, 1H), 7.47 (d, J = 8.2 Hz, 1H), 6.42 (d, J = 37.0 Hz, 2H), 4.31 (t, J = 6.5 Hz, 1H), 4.15 (d, J = 7.0 Hz, 1H), 3.12 (d, J = 9.8 Hz, 1H), 2.84 (dd, J = 12.4, 5.1 Hz, 1H), 2.65 (t, J = 7.4 Hz, 2H), 2.59 (d, J = 12.5 Hz, 1H), 1.75 – 1.58 (m, 4H), 1.55 – 1.32 (m, 2H) ppm.

^{13}C NMR (101 MHz, DMSO-d_6) δ 170.99, 162.72, 143.09, 135.56, 127.27, 125.62, 125.30, 119.55, 61.02, 59.20, 55.33, 37.04, 33.06, 28.00, 27.85, 24.11 ppm.

ESI-HRMS $[M+H]^+$ calcd.366.11 for $C_{16}H_{20}N_3O_5S^+$, found 366.11.

***N*-(2,2-dimethoxyethyl)-5-((3a*S*,4*S*,6a*R*)-2-oxohexahydro-1*H*-thieno[3,4-*d*]imidazol-4-yl)pentanamide (7)**

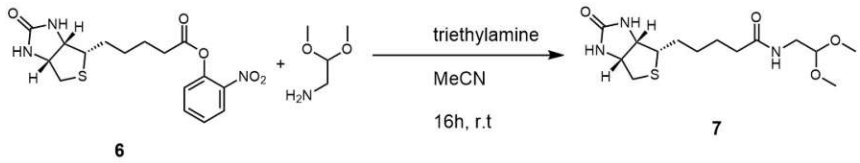

6 7

Compound **6** (1 eq., 84.0 mg, 0.23 mmol) was suspended in dry acetonitrile (4.5 mL), then 2,2-dimethoxyethan-1-amine (1.2 eq., 30.1 µL, 0.28 mmol) and triethylamine (1.2 eq., 38.5 µL, 0.28 mmol) were added. The yellow reaction was gently heated to dissolve the starting material, then it was stirred at r.t. under N_2 atmosphere for 16 h. The solvent was removed under reduced pressure and the product was purified by column chromatography (4 g silica, CombiFlash Rf+, 0-10% MeOH in DCM) leaving the product **7** (66.8 mg, 88%) as a white solid.

^{1}H NMR (500 MHz, DMSO-d_6) δ 7.86 (t, J = 5.9 Hz, 1H), 6.41 (s, J = 1.9 Hz, 1H), 6.35 (s, 1H), 4.35 – 4.27 (m, 2H), 4.12 (ddd, J = 7.8, 4.4, 1.9 Hz, 1H), 3.25 (s, 6H), 3.13 (t, J = 5.7 Hz, 2H), 3.11 – 3.05 (m, 1H), 2.82 (dd, J = 12.4, 5.1 Hz, 1H), 2.57 (d, J = 12.4 Hz, 1H), 2.08 (t, J = 7.4 Hz, 2H), 1.66 – 1.16 (m, 6H) ppm.

^{13}C NMR (126 MHz, DMSO-d_6) δ 172.28, 162.71, 102.07, 61.05, 59.20, 55.43, 53.21, 40.31, 39.78, 34.98, 28.15, 28.04, 25.27 ppm.

ESI-HRMS $[M+H]^+$ calcd. 354.15 for $C_{14}H_{25}N_3O_4SNa^+$, found 354.15.

Chapter 6

Literature

(1) Teng, M.; Gray, N. S. *Cell Chemical Biology* **2023**, *30*, 864–878.

(2) Schapira, M.; Calabrese, M. F.; Bullock, A. N.; Crews, C. M. *Nature Reviews Drug Discovery* **2019**, *18*, 949–963.

(3) Pickart, C. M.; Eddins, M. J. *Biochimica et Biophysica Acta (BBA) - Molecular Cell Research* **2004**, *1695*, 55–72.

(4) Yan, J.; Li, T.; Miao, Z.; Wang, P.; Sheng, C.; Zhuang, C. *Journal of Medicinal Chemistry* **2022**, *65*, 8798–8827.

(5) Ahn, G.; Banik, S. M.; Bertozzi, C. R. *Cell Chemical Biology* **2021**, *28*, 1072–1080.

(6) Wu, T.; Yoon, H.; Xiong, Y.; Dixon-Clarke, S. E.; Nowak, R. P.; Fischer, E. S. *Nature Structural & Molecular Biology* **2020**, *27*, 605–614.

(7) Weng, G.; Shen, C.; Cao, D.; Gao, J.; Dong, X.; He, Q.; Yang, B.; Li, D.; Wu, J.; Hou, T. *Nucleic Acids Research* **2021**, *49*, D1381–D1387.

(8) Weng, G.; Cai, X.; Cao, D.; Du, H.; Shen, C.; Deng, Y.; He, Q.; Yang, B.; Li, D.; Hou, T. *Nucleic Acids Research* **2023**, *51*, D1367–D1372.

(9) Hou, T. http://cadd.zju.edu.cn/protacdb/, 2024.

(10) Li, W.; Bengtson, M. H.; Ulbrich, A.; Matsuda, A.; Reddy, V. A.; Orth, A.; Chanda, S. K.; Batalov, S.; Joazeiro, C. A. P. *PLoS ONE* **2008**, *3*, e1487.

(11) Békés, M.; Langley, D. R.; Crews, C. M. *Nature Reviews Drug Discovery* **2022**, *21*, 181–200.

(12) Li, Y.-D. et al. *bioRxiv* **2023**, 2023.02.14.528208.

(13) Filippakopoulos, P. et al. *Nature* **2010**, *468*, 1067–1073.

(14) Shi, X.; Liu, C.; Liu, B.; Chen, J.; Wu, X.; Gong, W. *Die Pharmazie* **2018**, *73*, 491–493.

(15) Jang, S.-M.; Redon, C. E.; Aladjem, M. I. *BioEssays* **2021**, *43*, DOI: 10.1002/bies.202100057.

(16) Zhang, X.; Crowley, V. M.; Wucherpfennig, T. G.; Dix, M. M.; Cravatt, B. F. *Nature Chemical Biology* **2019**, *15*, 737–746.

(17) Pu, C.; Tong, Y.; Liu, Y.; Lan, S.; Wang, S.; Yan, G.; Zhang, H.; Luo, D.; Ma, X.; Yu, S.; Huang, Q.; Deng, R.; Li, R. *European Journal of Medicinal Chemistry* **2022**, *236*, 114321.

(18) Lim, M.; Cong, T. D.; Orr, L. M.; Toriki, E. S.; Kile, A. C.; Papatzimas, J. W.; Lee, E.; Lin, Y.; Nomura, D. K. *ACS Central Science* **2024**, DOI: 10.1021/acscentsci.4c00286.

(19) Ohba, K.; Niwa, Y.; Matsudaira, T.; Hamada, M.; Yamazaki, R.; Ibuki, T. Sulfonamide or sulfinamide compound having effect of inducing BRD4 protein degradation and pharmaceutical use thereof, 2021.

(20) Hsia, O. et al. *Nature* **2024**, *627*, 204–211.

(21) Ke, L.; Zhu, G.; Qian, H.; Xiang, G.; Chen, Q.; Chen, Z. *Organic Letters* **2019**, *21*, 4008–4013.

(22) Abdel-Magid, A. F.; Mehrman, S. J. *Organic Process Research & Development* **2006**, *10*, 971–1031.

(23) Pletz, J.; Berg, B.; Breinbauer, R. *Synthesis* **2016**, *48*, 1301–1317.

(24) Lu, J.; Qian, Y.; Altieri, M.; Dong, H.; Wang, J.; Raina, K.; Hines, J.; Winkler, J. D.; Crew, A. P.; Coleman, K.; Crews, C. M. *Chemistry & Biology* **2015**, *22*, 755–763.

(25) BroadPharm Protocol for Azide-Alkyne Click Chemistry, 2022.